Inquiry: The University of Arkansas Undergraduate Research Journal

Volume 16 Article 1

Spring 2014

Inquiry: The University of Arkansas Undergraduate Research Journal - Volume 16 - Spring 2014

Inquiry Editors

THE UNIVERSITY OF ARKANSAS UNDERGRADUATE RESEARCH JOURNAL

UNIVERSITY OF ARKANSAS

INQUIRY

Volume 16 Spring 2014

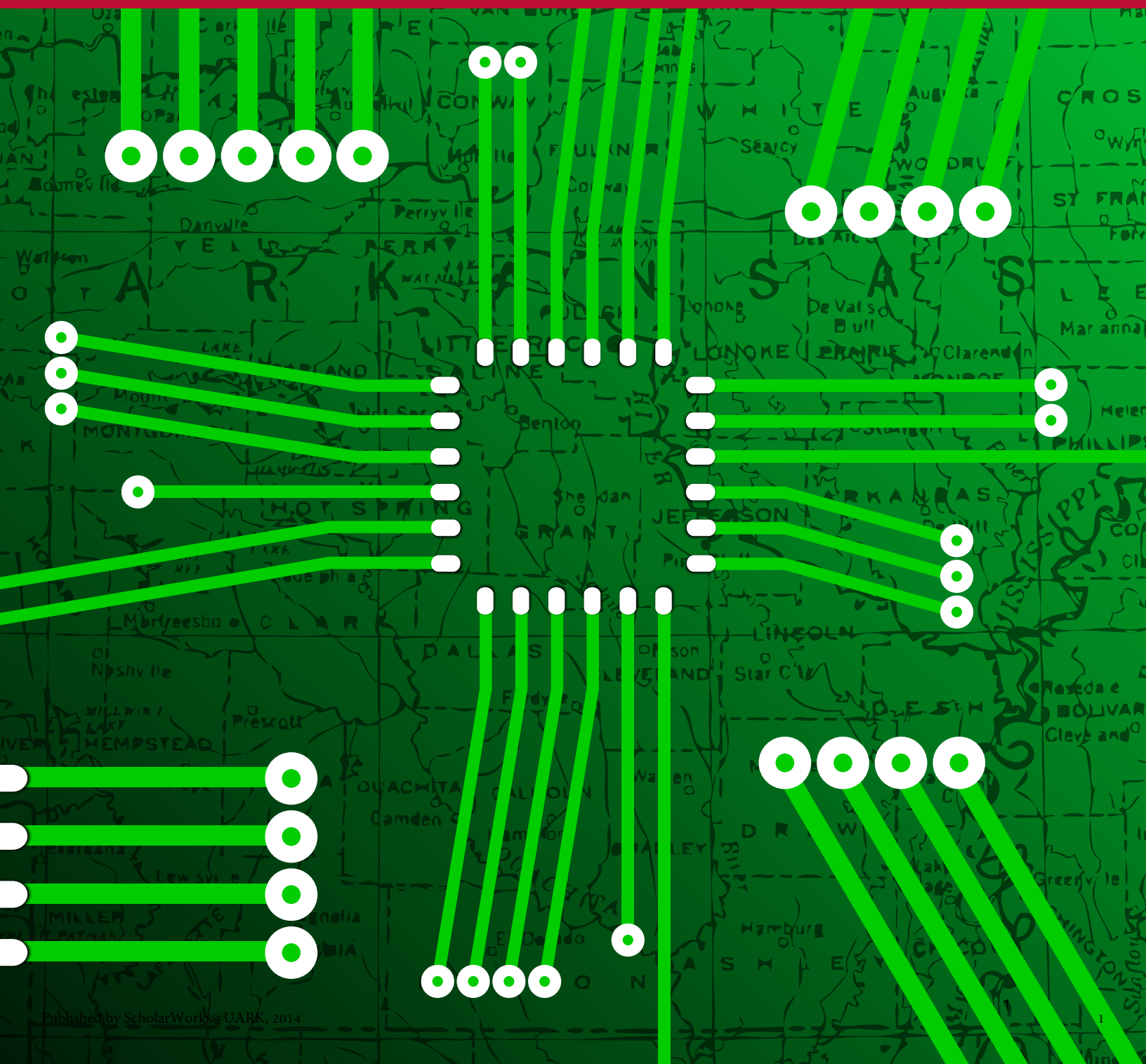

FOREWORD

Welcome to Volume 16 of the *Inquiry Undergraduate Research Journal.* The *Inquiry Journal* was developed by the Teaching Academy of the University of Arkansas and is supported financially and conceptually by the offices of the Provost and the Vice Provost for Research and Economic Development. *Inquiry* provides a forum for sharing the research and creative endeavors of undergraduate students and their faculty mentors at the University of Arkansas.

Volume 16 of the *Inquiry Undergraduate Research Journal* features the unique contributions of four undergraduate student authors and their faculty mentors. Their research and creative endeavors span diverse fields at the University of Arkansas, including Architecture, Biological Sciences, Horticulture and Food Sciences, and Mathematics. In her study, Sophie Hollenberg finds support for an innovative medical intervention to treat hospitalized patients infected with pseudomembranous colitis, a common bacterial infection. Bethany Sebesta examined the relationships between sensory and composition attributes of blackberry genotypes from the University of Arkansas Department of Agriculture breeding program in order to inform future breeding decisions. In the field of Mathematics, Raymond T. Walter provides a concise and complete explanation of a classical result of Liouville that every conformal map is a Möbius transform in Euclidean space of dimension at least three. Finally, Leniqueca Welcome, Architecture, provides a comprehensive analysis of the ways in which ornamentation was used on the exterior of residential homes to reflect a socio-political class system in 20th century Trinidad.

I would like to extend a special thank you to the many faculty members who volunteered their time and expertise to provide comprehensive reviews of student manuscripts. While we are unable to publish all of the submitted manuscripts, we want to thank the students and faculty mentors for their diligent efforts. Please join me in congratulating our authors; I hope that you enjoy this edition of the journal as much as we have.

We plan to publish Volume 17 of the *Inquiry* journal in September 2014. I encourage undergraduate students and faculty mentors to consider the *Inquiry Undergraduate Research Journal* for future publication.

Marcia A. Shobe, Editor

TABLE OF CONTENTS

***Inquiry Undergraduate Research Journal* of the University of Arkansas**

Volume 16 **Spring 2014**

Table of Contents

Cover image by Rob Byrd Designs

EFFECT OF THE *CLOSTRIDIUM DIFFICILE* TCDE PROTEIN ON MEMBRANES OF *ESCHERICHIA COLI*

By Sophie Hollenberg
Department of Biological Sciences

Faculty Mentor: David Mack Ivey
Department of Biological Sciences

ABSTRACT

Clostridium difficile infects millions of hospitalized patients worldwide, causing pseudomembranous colitis, a disease with symptoms attributable to two toxins produced by the bacterium. The PaLoc gene locus in the C. difficile genome is responsible for toxin production and activation, but it is not known how the toxins are released from the pathogen. Within PaLoc is a gene for the TcdE protein, which shares striking similarity to a class of membrane pore-forming proteins called holins. To assess whether TcdE catalyzes toxin release, the engineered tcdE gene was expressed in Escherichia coli. An arabinose promoter upstream of the tcdE gene was manipulated to modulate transcription of the gene. Recombinant E. coli cells showed viability and morphological changes, throughout different phases of growth, consistent with membrane pore formation. Thus, TcdE has the properties required of a toxin release mechanism, and drugs that block TcdE function could be candidates for drug therapy for treating infected patients.

Introduction

Among the *Clostridiaceae* family, the bacterium *Clostridium difficile* is the cause of a major nosocomial gastrointestinal infection in the United States, infecting up to 7,000 hospitalized Americans per day (Peery et al., 2012). The bacterium has been recognized as the most important isolated cause of hospital-acquired antibiotic-associated diarrhea and pseudomembranous colitis (Carroll & Bartlett, 2011). The typical risk factors involved with developing pseudomembranous colitis include long-term exposure to a health care environment, antibiotic prescription, and exposure to spores of the pathogen (Carroll & Bartlett, 2011). In addition, it is becoming more common to find a pregnant woman or young adult who has developed an infection due to *C. difficile* with the absence of risk factors (O'Connor, Johnson, & Gerding, 2009). Symptoms of infection range from an onset of antibiotic-associated diarrhea, or the development of pseudomembranous colitis, and in extreme cases, death.

C. difficile is a gram-positive anaerobe capable of producing spores that are resistant to many chemicals, heat, and even UV light (Carter, Rood, & Lyras, 2012). When patients are treated with certain antibiotics, the normal enteric bacteria are depleted, allowing *C. difficile* to infect (Borriello, 1998). Spores of the bacterium are transferred from the feces of infected patients and become commonplace in hospitals and nursing homes (Carroll & Bartlett, 2011). The spores are ingested and then pass through the upper alimentary tract to reach the lower gastrointestinal tract. Once residing in an appropriate environment, the now vegetative cells of *C. difficile* release toxins A and B that cause damage to the mucosal barrier and epithelial cells lining the gut (Carter et al., 2012). The ensuing cascade of cytokines and leukocytes may be responsible for the enhanced permeability, diarrhea, epithelial apoptosis, and ulceration of the digestive tract (Jafari et al., 2013).

The pathogenicity locus in infectious *C. difficile* has been termed PaLoc (Dupuy, Govind, Antunes, & Matamouros, 2008) (Figure 1). Containing five genes, it is solely responsible for transforming a nonvirulent strain of *C. difficile* into an infectious one (Govind & Dupuy, 2012).

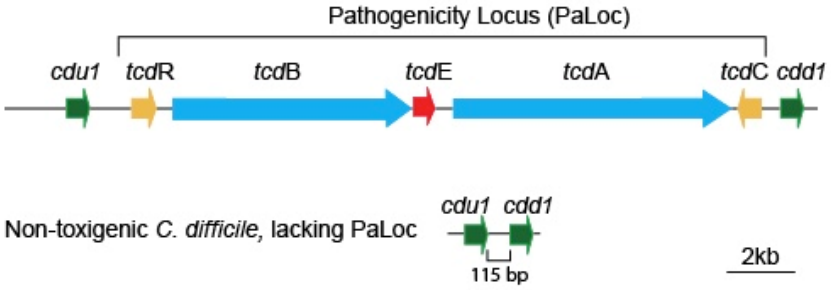

Figure 1. Toxigenic versus non-toxigenic C. difficile genomes. The toxigenic strain of C difficile contains the 19.6-kb pathogenicity locus PaLoc with five virulence genes. Non-toxigenic C. difficile contain a short 115bp sequence instead of the PaLoc locus (Govind & Dupuy, 2012).

Enterotoxins A and B are produced from the two genes in the PaLoc location called *tcdA* and *tcdB*. Their mechanism proceeds by glucosylation of the family of small Rho GTP-binding proteins, which disrupts the host cell cytoskeleton and leads to apoptosis (Carter et al., 2012). Since the PaLoc locus is wholly sufficient for virulence, there must exist a gene responsible for toxin release within this locus. One hypothesis is that *tcd*E is that gene, because of its homology to phage holin proteins (Govind & Dupuy, 2012). Bacteriophage lytic infections are characterized by an accumulation of holin proteins within lipid rafts in the plasma membrane, as shown in Figure 2 (Wang, Deaton, & Young, 2003). When a critical concentration of the holin monomers has been reached, an aqueous pore channel is thought to spontaneously form. The depolarization involved with the pore formation causes a conformational change within the holins, and they disperse to form the lesion shown in Figure 2 (Wang et al., 2003). Typically, endolysins accumulate in the cytoplasm until the critical point is reached, and a holin pore allows movement across the membrane. The membrane is then destroyed by degradation of murein (Govind & Dupuy, 2012).

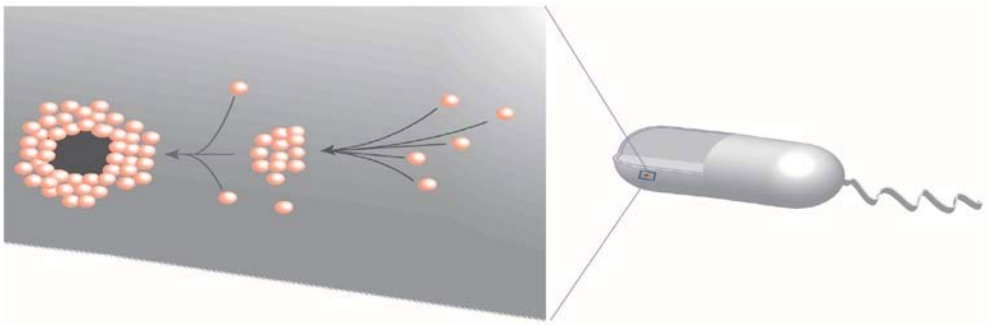

Figure 2. Pore formation by holing proteins. Each pink circle represents a holing protein. They are thought to accumulate until a critical concentration is reached, coinciding with formation of a port within the membrane.

In a study of the most frequent ribotypes of *C. difficile*, it was found that increased expression of the *tcdE* open reading frame had importance in the release of the toxins (Vohra & Poxton, 2011). Researchers induced cells to express the *tcdE* gene, and then visualized the effect with a transmission electron microscope (Tan, Wee, & Song, 2001). The results demonstrated a lack of membrane vesicles as well as fusion of the periplasm and cytosol in the cells with expressed *tcdE* gene. This evidence, compared to a control without *tcdE* expression, showed that the former cell was dying because of membrane disturbance. The authors posited that the fact that the *tcdE* gene is polycistronically transcribed with the *tcdA* and *tcdB* genes supports the critical pathogenic role of TcdE. Neither toxin A nor B have the capacity to allow for extracellular secretion, thus there must be another factor causing such excretion (Tan et al., 2001).

The full 19 kDa TcdE protein is suspected to be composed of three transmembrane helices that are depicted in Figure 3. The S^{105} is a form of the phage γ S protein that has holin activity, and is depicted to the left of the TcdE protein in Figure 3 (Govind & Dupuy, 2012). The similarities in structure contribute to the evidence for the holin activity of TcdE. In particular, it could be a member of the class I holins, of which phage γ S is a member. It has been demonstrated that the full 19 kDa translation product of *tcdE*, as shown in Figure 3, could be in

an inactive state (Olling et al., 2012). Previous *in vivo* experiments have suggested that the

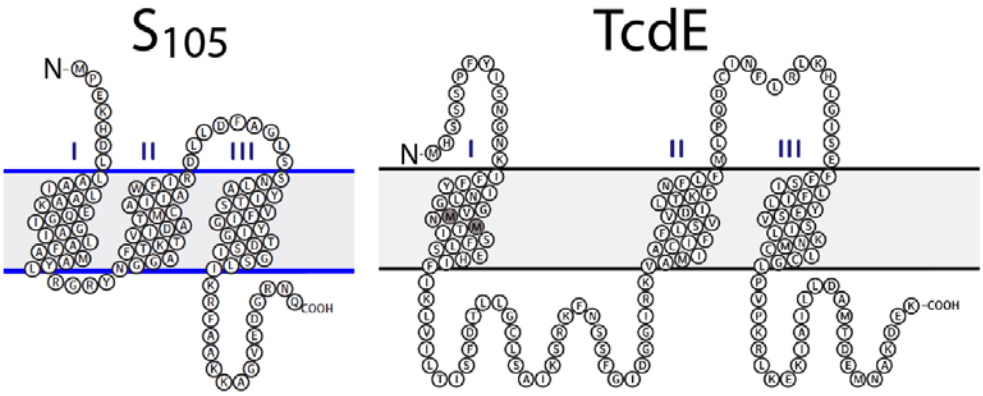

Figure 3. Structural similarity between TcdE and γ S holin protein. This illustration shows that the TcdE structure composed of three hydrophobic transmembrane domains is similar to the structure of a form of a phage γ S holin protein (Govind & Dupuy, 2012).

19 kDa TcdE isoform functions as an antiholin-like inhibitor of the smaller translation product, 16 kDa. So, this inhibition of the active isoform occurs until a precise time during which the functional holins, the 16 kDa isoform, are produced to initiate holin-mediated cell lysis. The 16 kDa TcdE isoform is thought to produce the holin activity, triggering membrane disruption by the formation of a pore through which toxins A and B may be released. The expression of the active 16 kDa isoform can occur by initiating translation at either of two alternative internal start codons, located at positions 72 and 79 of the *tcdE* open reading frame (Olling et al., 2012). These internal codons are depicted in Figure 4, along with the first start codon that may be used to create the entire 19 kDa inactive isoform.

Figure 4. N-terminal section of TcdE DNA. The DNA sequence harbors three alternative start codons that are shown in the figure. The first methionine codon may be translated to produce the 19 kDa isoform of TcdE (thought to be the inactive, regulated form). The interior alternative start codons located at positions 73 and 79 of the open reading frame may also be start points for translation, thus creating the suspected active holin 16kDa isoform of TcdE (Olling et al., 2012).

Since persistent antibiotic treatment is not always effective in treating patients infected with *C. difficile*, and is in fact a source of the infection, the search for a proper treatment is a priority. Currently, the standard approach is to discontinue antibiotic therapy, and instead prescribe a different antibiotic. Although this method reduces symptoms initially, there is a 20-25% chance that the patient will suffer a relapse of symptoms (Surawicz et al., 2000). The development of useful drugs has been impeded by the ambiguity surrounding the mechanism by which toxins are released. If the theory behind the holin activity of the TcdE protein in *C. difficile* is proved correct, then significant advances toward treatment of antibiotic-associated diarrhea and pseudomembranous colitis can be made. Therefore, the primary goals of the present study were to analyze the morphological effects that gradual amounts of both the inactive and active TcdE protein have on host cell membranes, and to create a growth curve consistent with bacterial growth and subsequent synthesis of TcdE proteins.

Materials and Methods

Media and growth conditions

The *E. coli* strains BL21 [pLysS] (*F⁻ ompT gal dcm lon hsdSB(rB- mB-)* λ(DE3) pLysS(CmR)) and UA381, a chloramphenicol-resistant derivative of *E. coli* BL21 star (*F⁻ ompT gal dcm lon hsdSB(rB- mB-) rne*131 λ(DE3) pRARE), were maintained on Luria-Bertani (LB) broth and agar supplemented with chloramphenicol at 30 µg/ml. Plasmids used in this study conferred ampicillin resistance, and were selected with ampicillin (100 µg/ml) or carbenicillin (50µg/ml).

Recombinant DNA procedures

DNA purification, restriction endonuclease digestions, ligations, transformations with chemically competent cells, and polymerase chain reaction (PCR) was performed using standard

molecular biology methods (Bouillaut, McBride, & Sorg, 2011). Electroporation employed a Bio-Rad Gene Pulser apparatus, set to deliver 1.7 kV at 200 ohms and 25 µfarads. Electroporated cells were incubated with shaking at 37^{o}C for 1 hour prior to plating. Site-directed mutagenesis was performed using the Quickchange kit from Agilent (Santa Clara, CA).

Construction of the arabinose-inducible tcdE gene

A pGEM5Zf(+)-based plasmid containing the promoter-less *tcdE* gene, made in previous studies and designated pUA573, was used to insert the gene into the pBAD-HisA plasmid. Plasmid pUA573 was cut with restriction enzymes NcoI and HindIII, around the *tcdE* gene, thus isolating the linear *tcdE* fragment. The *tcdE* fragment was then added to NcoI/HindIII-treated pBAD-HisA, and recombinant plasmid was ligated in such a way that the *tcdE* gene was under the control of the arabinose promoter. The resultant plasmid is referred to as pUA575. The plasmid pUA575 was then transformed into *E. coli* strain UA381, a BL21-based strain suitable for expression studies. The transformed product is referred to as strain UA577.

To test the importance of the two potential internal start codons in the *tcd*E gene, a mutant form of strain UA577 was made. The mutant plasmid was made via site-directed mutagenesis. The Quikchange procedure was utilized to mutate the internal alternative start codons from the start codon methionine (AUG) to the codon ACG. The mutated plasmid transformed in the UA381 *E. coli* strain is referred to as UA585.

Induction of arabinose promoter

Various concentrations of the monosaccharide L-arabinose were made by diluting a 10% stock into LB broth. The final concentrations were 2%, 0.2%, 0.02%, 0.002%, and 0.0002%. Cultures to be induced were shaken at 37°C until they were at the beginning of the log phase of growth. Ten milliliters of the cultures were aliquoted into each of five tubes, and 100 µl of each

arabinose concentration was added to the tubes. The tubes were then shaken at 37°C, and samples were analyzed tubidimetrically and by fluorescence microscopy at various time points after arabinose addition.

Microscopy

Slides prepared by wet mount or by pipetting cells onto agarose pads were examined by phase contrast and fluorescence microscopy, using a Zeiss Axio Imager M1 microscope.

Results

The primary aim of the present study was to assess the effect that the TcdE protein has on the cell membranes of *E. coli* cells. Because the likely effect of high levels of expression of a holin-like protein is cell lysis, it proved necessary to control the dosage of TcdE in order to obtain viable *E. coli* cells. The route determined to be the most effective involved the use of the arabinose promoter of plasmid pBAD/HisA, in a host *E. coli* strain derived from the BL21 (DE3) strains typically used for T7 promoter-driven expression. The arabinose promoter should not allow transcription of the *tcdE* gene whatsoever until there is a sufficient amount of arabinose present (Khlebnikov, Risa, Skaug, Carrier, & Keasling, 2000). We used this arabinose-inducible system to study the effect of TcdE expression on host *E. coli* cells. First, we measured the optical density of an exponentially growing culture of *E. coli* cells both before and after the addition of varying concentrations of arabinose (see Methods). We found that increasing arabinose concentrations decreased culture turbidity (Figure 5), suggesting the TcdE expression may be causing cellular lysis. Cells containing the control plasmid pUA579, lacking the *tcdE*

gene, showed no change in turbidity with increasing arabinose concentrations, suggesting that the effect was indeed due to TcdE expression.

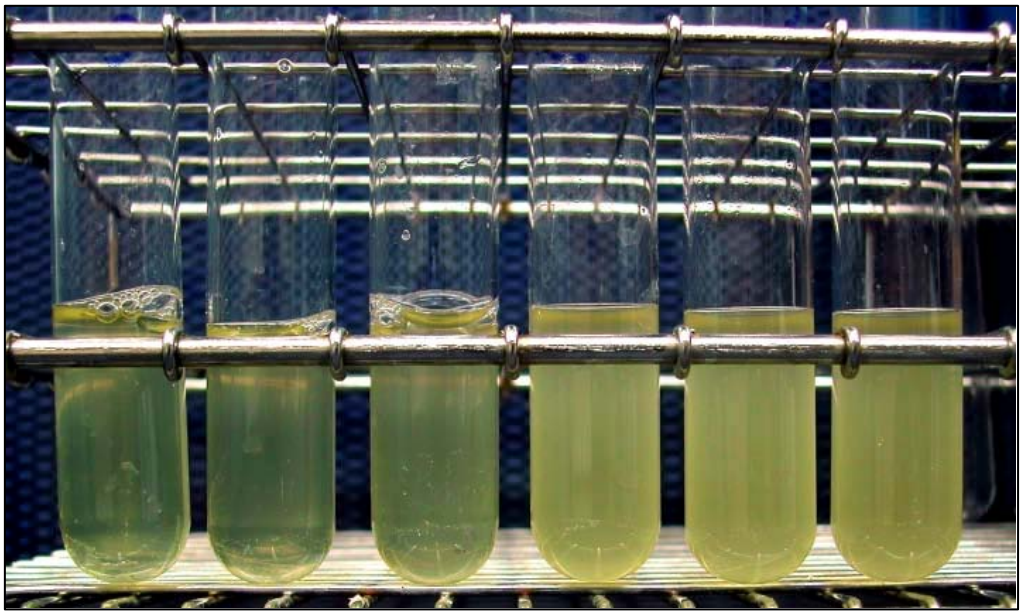

Figure 5. Turbidity decreases of strain UA577, associated with varying arabinose concentrations. In the five left-most tubes, arabinose concentrations decrease as a 10-fold serial dilution, left to right, from 2% to 0%. The tube on the far right contains cells the tcdE-minus control plasmid, exposed to 2% arabinose.

In order to have a more quantitative assessment the difference in growth between cells that express the putative holin protein versus cells that do not, growth curves were constructed of cells containing the wild-type and mutant *tcd*E alleles. For UA577 cells expressing wild-type *tcdE*, adding 0.2% arabinose to mid-log phase cells causes an immediate decline in cell number. The decline persists for approximately 1 hour, after which the cell numbers remain constant for at least another 4 hours. Based on comparisons of turbidity, the arabinose-treated cultures are estimated to have an 80% reduction in the number of intact cells relative to untreated cultures. Arabinose at 0.002%, which likely induces lower levels of expression of *tcdE*, causes a less pronounced decline in cell numbers, and turbidity begins to increase toward the end of the 4-hour induction period. In contrast, UA585 cells expressing the mutated *tcdE* gene do not show a

significant decline in cell numbers in response to arabinose, at even the highest concentration (0.2%). Low concentrations (0.002%) have almost no effect on growth, while 0.2% arabinose triggers a slight decrease in growth rate during the first hour of induction, followed by a 3-4 hour period during which the cell population remains constant or increases slightly.

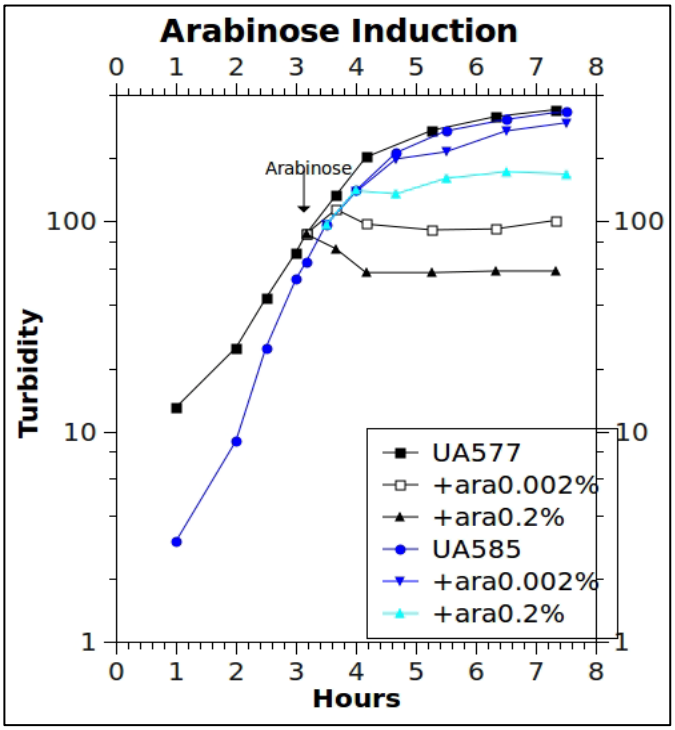

Figure 6. Effects of arabinose induced expression of wild-type and mutant tcdE alleles on *E. coli* growth.

Next, we visually inspected *E. coli* cells expressing TcdE when exposed to these various amounts of arabinose. This approach allowed us to examine cellular morphology to better understand why TcdE expression decreased turbidity. As a control, we also used a mutant allele of *tcdE*, where two internal methionine codons were changed to threonine codons. This mutant allele is unable to produce the active 16 kDa isoform, as a result of disrupting the alternative translation initiation sites at the internal methionine/start codons. We examined *E. coli* carrying either wild-type or mutant *tcdE* following the addition of 0.002% arabinose. Cells were visualized 1 and 2 hours after arabinose addition (Figure 7). Cells expressing wild-type *tcdE*

following 1-hour induction with 0.002% arabinose were mostly the characteristic *E. coli* rod

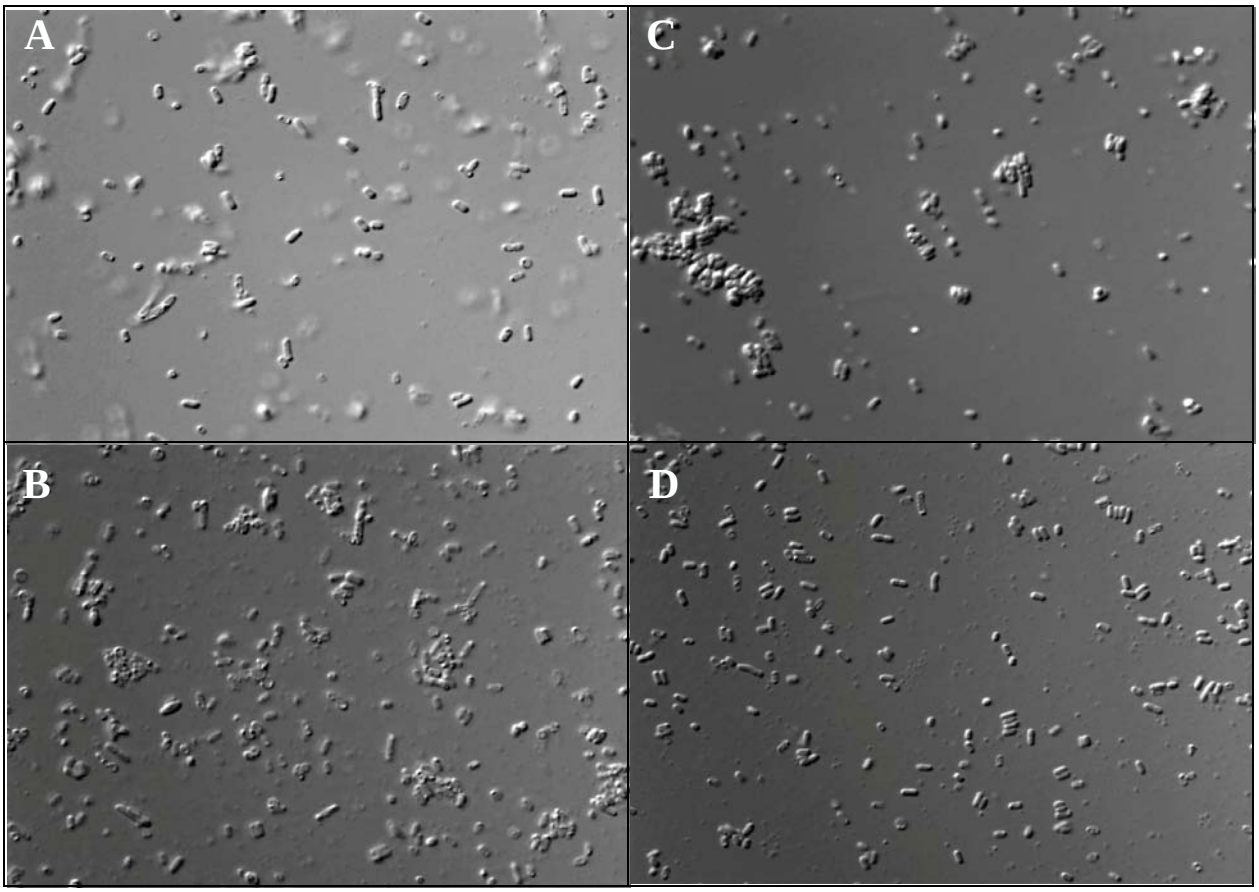

Figures 7A-7D. A) Wild-type UA577 one hour after induction with arabinose of concentration 0.002%. B) Wild-type UA577 two hours after induction with arabinose concentration of 0.002%. C) Mutant UA585 one hour after induction with arabinose of concentration 0.002%. D) Mutant UA585 two hours after induction with arabinose of concentration 0.002%.

shape, with some cells having a rounded or oval shape. A 2-hour induction led to a higher percentage of rounded cells (Figure 7B). At higher magnification the cells show a clumping of rounded, enlarged, less opaque morphology.

The control cells containing the mutant *tcdE* allele (which only can translate the 19 kDa isoform) were also exposed to 0.002% arabinose and visualized microscopically (Figure 7). Figure 7C shows the *E. coli* cells one hour after induction with arabinose, which demonstrates a characteristic clumping of the *E. coli* cells. In contrast with the wild-type form, they are almost

all the typical rod-shaped *E. coli* cells. After an additional hour, more isolated *E. coli* cells can be seen in Figure 7D that retain their characteristic rod shape more so than the wild-type strain that had been exposed to the same amount of arabinose and after the same length of time (Figure 7B).

The morphological differences due to the effect of adding arabinose to the wild-type versus mutant cells can be better seen in magnifications. This was done with the cells exposed to 0.002% arabinose two hours prior to visualizing them under the microscope (Figure 8).

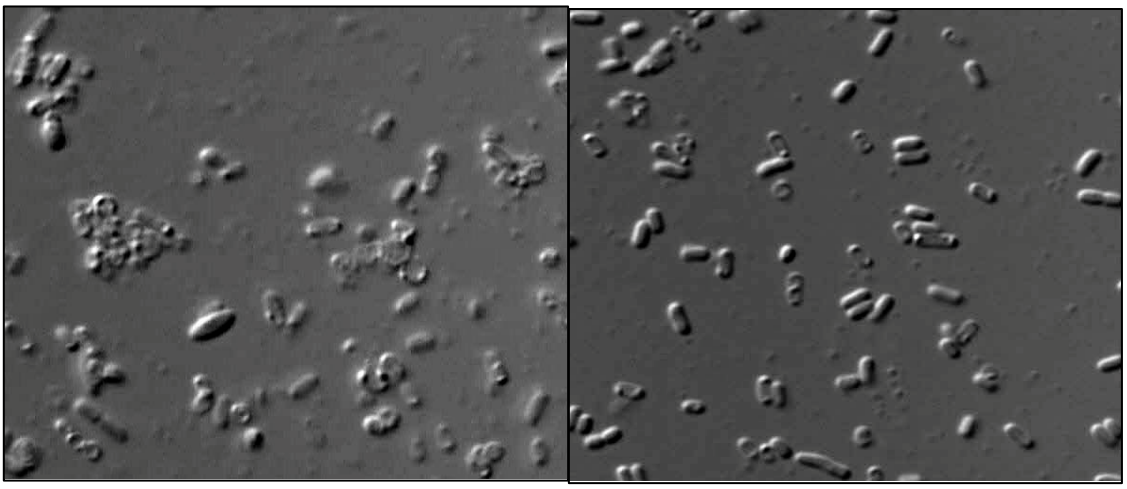

Figure 8. Magnified image of *E. coli* cells containing A) the wild-type *tcd*E gene or B) the mutant *tcd*E allele, each exposed to 0.002% arabinose for two hours.

We also used fluorescence microscopy to directly compare morphological differences between cells containing wild-type versus mutant *tcdE*. Arabinose induction was performed on cells containing *tcdE*, along with an *E. coli* strain expressing green fluorescent protein (GFP), but lacking *tcd*E. Fluorecent and phase contrast images of each field were superimposed to compare the differences in cell shape. GFP-containing cells showed the typical morphology of log-phase *E. coli*, while the non-fluorescent cells were larger and mostly flattened or otherwise misshapened (Figure 9). The results show that the dramatic morphological changes seen in reponse to arabinose induction were the result of TcdE protein accumulation, and not simply caused by activation of the arabinose promoter *per se*.

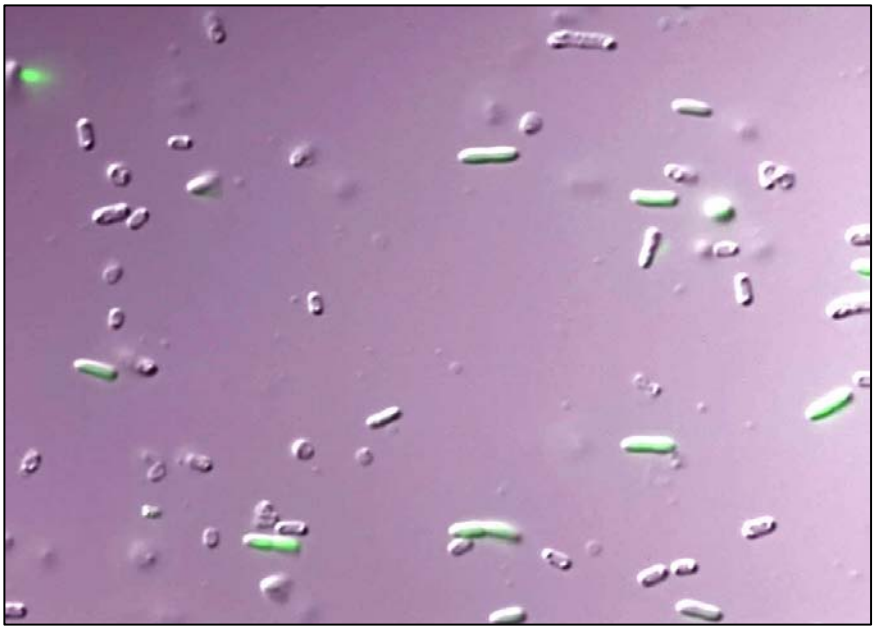

Figure 9. Superimposed fluorescence and phase constrast image of arabinose-treated *E. coli* cells. GFP containing cells do not contain the *tcd*E gene.

Discussion

An essential feature in future drug developments for pseudomembranous colitis and antibiotic-associated diarrhea is to understand the mechanism by which toxins A and B are released from *C. difficile*. The TcdE protein could be targeted in drugs developed for treating these nosocomial diseases if it can be identified as the source by which the symptom-carrying toxins are released. An additional topic of interest with regards to drug development is the potential inhibitory function that the 19 kDa isoform of the TcdE protein may possess. The progress of such drug development is a priority within the medical community due to the ineffectiveness of current therapy. Existing antibiotics are actually both part of the source of the disease and the treatment for it. Although different types of antibiotics are prescribed following infection by *C. difficile*, this therapy does not prove to be sustainable with recurrance of symptoms occuring one fourth of the time, and within two to three weeks after discontinuing the original antibiotic (Kelly & LaMont, 1998).

Overall, the results of the present study support the prediction that there would be alterations or disruption to the plasma membrane of host cells that express the TcdE protein (Tan et al., 2001). The modulated induction of the arabinose promoter that was used for expressing the *tcdE* gene proved to be effective. Such expression has proved to be a problem in the past when excessive amounts of TcdE would lyse the cells and no analyses could be made on the host cells (Tan et al., 2001). The effect of *tcdE* expression on growth, as measured by turbidity, suggests that wild-type TcdE protein expression causes dose-dependent lysis of cells. It is likely that a threshold concentration of TcdE proteins is required in order for permanent damage to the cytoplasmic membrane to occur. Lower levels of induction of the wild-type *tcdE* gene, or even high levels of induction of the mutated *tcdE* gene, lead to fewer cells with the threshold concentration of TcdE protein. In those cases, the effects on turbidity and cell morphology are less pronounced, and/or require longer incubations in order to be observed.

The morphology of the wild-type cells compared to the mutant cells after induction with arabinose also presented substantial evidence for the role that TcdE plays in the state of the host membrane. As demonstrated with the use of microscopy, the wild-type cells exhibited an unusual round shape that is very different than the mutant strain that retained the rod-shape typical of *E. coli* cells. The wild-type cells also presented a more translucent form, being less opaque and generally more hazy in appearance compared to the distinct mutant cells that had viable, intact membranes. This phenomenon could possibly be explained as being due to the disruption of wild-type membranes. Another study (Tan et al., 2001) produced similar results showing a lack of membrane vesicles, merging of the cytosol and periplasm, and membrane foldings in the cells expressing TcdE. Compared to the control that had no TcdE expressed, it maintained a differentiated cytosol and periplasm and a distinct, smooth membrane outline. This is what was

seen in the mutant *E. coli* cells in the present study, while the less opaque membrane outline of the wild-type strain could be due to similar reasons that the researchers previously discovered.

The wild-type UA577 cells also demonstrated an increase in clustering at the two hour mark after arabinose induction while the mutant cells were individually isolated from each other. A potential explanation for this finding could be due to the clustering that holin proteins undergo prior to pore formation and holin lesion. Most of the clustered cells also have the irregular shape previously discussed, so these wild-type cells could be aggregating and also undergoing membrane disruption due to the holin lesion whereas the mutant cells that have the inactive TcdE protein could be retaining their morphology and spatial independence.

These studies suggest that potential source of drug advancement could be aimed at the oligimerization of the holin-like TcdE proteins. If the proteins are unable to congregate and interact, then they could not oligomerize and create the pore in the membrane that ultimately leads to release of toxins A and B, causing symptoms of pseudomembranous colitis and antibiotic-associated diarrhea. In order to progress in this direction, however, the TcdE protein must be confirmed as a holin protein. Future studies designed to directly test the holin function of TcdE include the construction of His/3XFlag-tagged TcdE. If such a protein, bound to fluorescent antibodies, exhibits a clustering or halo shape, then such a finding would contribute to evidence supporting the holin theory of TcdE.

References

Borriello, S. P. (1998). Pathogenesis of Clostridium difficile infection. *Journal of Antimicrobial Chemotherapy*, *41*, 13–19.

Bouillaut, L., McBride, S. M., & Sorg, J. A. (2011). Genetic manipulation of Clostridium difficile. *Current Protocols in Microbiology*, *Chapter 9*, Unit 9A.2.

Carroll, K. C., & Bartlett, J. G. (2011). Biology of Clostridium difficile: Implications for epidemiology and diagnosis. *Annual Review of Microbiology*, *65*, 501–521.

Carter, G. P., Rood, J. I., & Lyras, D. (2012). The role of toxin A and toxin B in the virulence of Clostridium difficile. *Trends in Microbiology*, *20*(1), 21–9.

Dupuy, B., Govind, R., Antunes, A., & Matamouros, S. (2008). Clostridium difficile toxin synthesis is negatively regulated by TcdC. *Journal of Medical Microbiology*, *57*, 685–689.

Govind, R., & Dupuy, B. (2012). Secretion of Clostridium difficile toxins A and B requires the holin-like protein TcdE. *PLoS Pathogens*, *8*(6), e1002727.

Jafari, N. V., Kuehne, S. A., Bryant, C. E., Elawad, M., Wren, B. W., Minton, N. P., … Bajaj-Elliott, M. (2013). Clostridium difficile modulates host innate immunity via toxin-independent and dependent mechanism(s). *PloS One*, *8*(7), e69846.

Kelly, C. P., & LaMont, J. T. (1998). Clostridium difficile infection. *Annual Review of Medicine*, *49*, 375–390.

Khlebnikov, A., Risa, O., Skaug, T., Carrier, T. A., & Keasling, J. D. (2000). Regulatable arabinose-inducible gene expression system with consistent control in all cells of a culture. *Journal of Bacteriology*, *182*(24), 7029–7034.

O'Connor, J. R., Johnson, S., & Gerding, D. N. (2009). Clostridium difficile infection caused by the epidemic BI/NAP1/027 strain. *Gastroenterology*, *136*(6), 1913–1924.

Olling, A., Seehase, S., Minton, N. P., Tatge, H., Schröter, S., Kohlscheen, S., … Gerhard, R. (2012). Release of TcdA and TcdB from Clostridium difficile cdi 630 is not affected by functional inactivation of the tcdE gene. *Microbial Pathogenesis, 52*(1), 92–100.

Peery, A. F., Dellon, E. S., Lund, J., Crockett, S. D., McGowan, C. E., Bulsiewicz, W. J., … Shaheen, N. J. (2012). Burden of gastrointestinal disease in the United States: 2012 update. *Gastroenterology, 143*(5), 1187–1179.

Surawicz, C. M., McFarland, L. V., Greenberg, R. N., Rubin, M., Fekety, R., Mulligan, M. E., … Elmer, G. W. (2000). The search for a better treatment for recurrent Clostridium difficile disease: Use of high-dose vancomycin combined with Saccharomyces boulardii. *Clinical Infectious Diseases, 31*(4), 1012–1017.

Tan, K. S., Wee, B. Y., & Song, K. P. (2001). Evidence for holin function of tcdE gene in the pathogenicity of Clostridium difficile. *Journal of Clinical Microbiology*, *50*, 613–619.

Vohra, P., & Poxton, I. R. (2011). Comparison of toxin and spore production in clinically relevant strains of Clostridium difficile. *Microbiology, 157*, 1343–1353.

Wang, I.-N., Deaton, J., & Young, R. (2003). Sizing the holin lesion with an endolysin--galactosidase fusion. *Journal of Bacteriology*, *185*(3), 779–787.

DESCRIPTIVE SENSORY ANALYSIS AND COMPOSITION OF BLACKBERRY GENOTYPES

By Bethany Sebesta
Departments of Horticulture and Food Science

Faculty Mentors:
Dr. John R. Clark, Department of Horticulture
Dr. Luke Howard, Department of Food Science
Dr. Renee Threlfall, Institute of Food Science and Engineering

Abstract

Consumer interest in blackberries has been increasing due in part to reputed health-promoting factors. Appearance, flavor, and texture attributes of blackberry fruits are important to consumers. The objective of this study was to investigate correlations among sensory and composition attributes of blackberry genotypes from the University of Arkansas Division of Agriculture breeding program. Descriptive panelists evaluated attributes of 20 blackberry genotypes. Composition attributes were evaluated for these and two additional genotypes. 'Natchez' had the most pyrenes/berry and the highest levels of total ellagitannins. Selection A-2215 was scored highest for descriptive-evaluated sweetness and had the highest soluble solids content. Total ellagitannins ($r= 0.57$; $p<0.0095$) and ORAC ($r= 0.54$; $p<0.0146$) were moderately correlated to seediness, which may reflect the value of ORAC factors in pyrenes. These initial investigations of the relationship between sensory and composition of blackberry genotypes provide insights that can be used for future blackberry cultivar assessments.

Introduction

Blackberries are a high-value horticultural crop and are grown worldwide for both the fresh market and for processing. Blackberries are classified in the *Rosaceae* family and *Rubus* genus (Finn & Clark, 2012). The blackberry fruit is an aggregate fruit comprised of drupelets surrounding the soft tissue receptacle or torus. The size of a blackberry fruit is determined by the combination of drupelet number and size (Clark, Stafne, Hall, & Finn, 2007). An individual drupelet includes a thin exocarp, a fleshy mesocarp, and a hard, lignified endocarp, also known as a pyrene, which encloses a single seed (Tomlik-Wyremblewska, Zieliński, & Guzicka, 2010). Pyrene physical characteristics are distinctive to each blackberry genotype and have been classified into the following three groups: straight, concave, or convex (Wada, Nonogaki, & Reed, 2010; Wada & Reed, 2010). Slight variation of pyrene shape can occur in the same genotype and the outer layer of the endocarp typically will have characteristic patterns of hollows (Tomlik-Wyremblewska et al., 2010). Pyrene shape and endocarp thickness influence perceived seediness when consumed (Takeda, 1993).

Not until the late 1990s were fresh blackberries readily available in retail markets in the United States (Clark, 2005; Strik, Clark, Finn, & Bañados, 2007). Since then, blackberries have established a more prominent place in the market due to enhanced shipping capability, prolonged shelf life, off-season availability, and double blossom/rosette disease resistance (Clark, 2005; Strik et al., 2007). In 2005, worldwide blackberry area was 20,036 ha and was projected to increase to over 27,000 ha by 2015 (Strik et al., 2007).

The increase in production area can in part be contributed to blackberry breeding programs. Blackberry breeding initiatives can be found on every continent with the exception of Antarctica (Strik et al., 2007). Blackberry breeding programs have existed for more than 100

years in the United States and continually strive to enhance favored qualities and to reduce undesirable traits. The first blackberry breeding program was initiated in 1909 at the Texas Agricultural Experiment Station (Clark & Finn, 2008). The oldest currently active program is located at the United States Department of Agriculture-Agricultural Research Service at Corvallis, OR; it was initiated in 1928 (Clark & Finn, 2008; Finn & Clark, 2012). In 1964, the University of Arkansas System Division of Agriculture (UASDOA) blackberry breeding program was initiated by Dr. James N. Moore (Clark, 1999). This effort, based at the UASDOA Fruit Research Station, Clarksville, AR, prioritized development efforts on attributes including thornlessness, erect growth habit, mechanical harvesting capability, disease resistance, productivity, and environmental and geographic adaptation (Clark, 1999; Clark & Finn, 2008). The fruit improvement objectives included large fruit size, good flavor, firmness, and high fertility (Clark, 1999). The UASDOA breeding program has expanded to focus on primocane-fruiting genotypes that produce fruit on first-year canes in addition to traditional second-year floricanes resulting in the commercial release of Prime-Jim®, Prime-Jan®, and Prime-Ark® 45 (Clark & Finn, 2008). Even though breeding priorities vary, most blackberry breeding programs focus on promoting consumption through improved fruit quality (Finn & Clark, 2012).

The processing industry prefers blackberries that have intense flavor and color, low pH, high soluble solids content and titratable acidity levels, low perceived seediness, and small pyrene size (Clark et al., 2007; Clark & Finn, 2008; Hall, Stephens, Stanley, Finn, & Yorgey, 2002). Of the Arkansas-released cultivars, ‘Choctaw’ has the smallest pyrene size (Clark, 1999); ‘Navaho’ and ‘Ouachita’ have higher soluble solids content (Clark et al., 2007; Clark & Finn, 2008); ‘Navaho’ is commonly sold to processors and is popular in United States fresh markets (Wada & Reed, 2010).

Some blackberry genotypes have been evaluated for nutraceutical/antioxidant levels (Cho, Howard, Prior, & Clark, 2004; Clark & Finn, 2008; Clark, Howard, & Talcott, 2002; Connor, Finn, & Alspach, 2005; Siriwoharn, Wrolstad, Finn, & Pereira, 2004). Blackberries are excellent sources of nutraceutical-rich polyphenolic compounds in the human diet (Reyes-Carmona, Yousef, Martinez-Peniche, & Lila, 2005; Sellappan, Akoh, & Krewer, 2002; Wang, Xu, & Jin, 2009; Zheng & Wang, 2003). High levels of anthocyanin, a polyphenolic antioxidant, naturally occur in blackberries (Clark et al., 2007) and account for the dark red pigmentation of the fruit (Wang et al., 2009). Polyphenols, including anthocyanin, proanthocyanids, flavonones, and flavonols, have been shown to have protective effects against some human health diseases (Ness & Poulens, 1997; Prior et al., 1998; Reyes-Carmona et al., 2005; Steinmetz & Potter, 1996; Van der Sluis, Dekker, De Jager, & Jongen, 2001). Antioxidants are able to reduce free radicals in the human body (Liu, 2003; Narayana, Reddy, Chaluvadi, & Krishna, 2001; Reyes-Carmona et al., 2005; Sariburun, Şahin, Demir, Türkben, & Uylaşer, 2010). Potential beneficial effects of polyphenols include anti-inflammatory, antiviral, antimicrobial, and antioxidant activity (Reyes-Carmona et al., 2005). Anti-cancer properties can be attributed to phenolic compounds in berries (Sariburun et al., 2010; Seeram et al., 2006; Seeram, 2008). These potential nutraceutical components can impact the fruit quality and sensory perception.

Fruit qualities such as sweetness, tartness, flavor, and astringency along with color, firmness, and seediness are important to consumers whether the berries are processed or consumed fresh (Clark & Finn, 2008). In general, consumers prefer fresh blackberries that are perceived as less “seedy” (i.e. fewer pyrene number or smaller size). The structure, size, and number of pyrenes in the blackberry may influence mouthfeel of the blackberries when consumed (Clark et al., 2007). Small pyrene size (< 3 mg) is preferred in both fresh-market and

processed blackberry products, and large pyrenes can be objectionable (Moore, Lundergan, & Brown, 1975). Moore et al. (1975) also found that pyrene size in blackberries is highly heritable with partial dominance for small pyrene size. Fresh-market blackberries can feel "seedy" when consumed, depending on the pyrene attributes. Large pyrene size, based on weight, length, or volume, and seediness are also undesirable in processed blackberry products (Takeda, 1993). Yet, the proportion of pyrene weight to total berry weight is more important than pyrene size (Darrow & Sherwood, 1931). Pyrene weight and pyrene number were positively correlated with blackberry fruit weight (Moore, Brown, & Brown, 1974).

Although studies on blackberry pyrene characteristics and morphology have been published, there is limited information on descriptive sensory analysis of Arkansas-developed fresh blackberries and the composition attributes that affect sensory scoring. The objective of this study was to investigate the descriptive sensory attributes and composition of blackberry genotypes from the UASDOA blackberry breeding program.

Materials and Methods

Fruit

Blackberry fruits were hand-harvested from the UASDOA Fruit Research Station, Clarksville, AR in 2012. The cultivars and genotypes 'Ouachita', 'Natchez', 'PrimeArk® 45', APF-190, A-2434, A-2312 ('Stella'), and APF-227 were harvested on 29 May; 'Ouachita', A-2108, 'Osage', A-2215, APF-156, APF-185, APF-205, and A-2473 were harvested on 7 June; and 'Ouachita', A-2252, A-2316, A-2418, A-2416, A-2419, 'Navaho', and 'Apache' were harvested on 14 June. After harvest, the berries were transported to the Food Science Department, University of Arkansas, Fayetteville, AR. In addition, blackberries were purchased commercially including 'Tupy' (Naturipe, Salinas, CA; fresh-market blackberries imported from

central Mexico) and commercial frozen blackberries (Great Value, Wal-Mart Stores, Inc. Bentonville, AR; cultivar unknown).

Sensory Descriptive Analysis

Descriptive sensory analysis of the fresh blackberries was performed at the Sensory and Consumer Research Center at the University of Arkansas, Fayetteville, AR. Trained descriptive panelists (n=8) participated in a 3-hour orientation session where the descriptive ballot was developed through consensus. The commercial frozen blackberries were thawed and used as the reference sample. Scores for the reference sample were also determined through consensus.

The fruits were evaluated on the same day they were harvested. 'Apache' and A-2252 were not sensory-evaluated because of limited quantity. Due to scheduling conflicts with the panelists on the multiple harvest dates, only four descriptive panelists (n=4) evaluated all the genotypes in the study.

Panelists (n=4) evaluated each blackberry genotype in duplicate using Spectrum® methods. The Spectrum® method is an objective method for describing the intensity of the blackberry fruit attributes. Descriptive panelists were trained with an absolute scale anchored by a specific reference. They assessed each attribute per genotype and replication at a particular intensity according to the reference points on the universal scale. Serving order was randomized across replication to prevent presentation order bias. The blackberry genotypes were served sequentially in 60 mL (2 oz) cups and were assigned random three-digit blinding codes. The blackberries were served at room temperature. Panelists were instructed to cleanse their palettes with unsalted crackers and water between samples. Expectorant cups were also provided. For each panelist, one paper ballot was completed per genotype for each replication.

The panelists identified and evaluated color/appearance, flavor by mouth, and texture attributes on a 10-point scale ranging from 0 (*less of the attribute*) to 9 (*more of the attribute*) in terms of intensity. The descriptive panel evaluated the color/appearance attribute [overall color intensity from 0 (*light red*) to 9 (*black*)], flavor attributes (overall flavor intensity, sweetness, and sourness), and the texture attribute (overall seediness) of the berries. The commercial frozen blackberries were thawed and used as a reference during each session. During orientation, scores for the reference sample were determined through consensus (overall color intensity = 4, overall flavor intensity = 4, sweetness = 2, sourness = 7, and overall seediness = 7), and the reference samples were used during the evaluation of the genotypes.

Composition Analysis

All evaluations for composition of blackberries were conducted at the Grape and Wine Research Laboratory, Department of Food Science, University of Arkansas, Fayetteville, AR. Three samples of approximately 100 g of berries were collected for each cultivar or genotype, placed in plastic storage bags, and stored at -20°C until analyses.

Berry and pyrene attributes. From the frozen berries, three berries per genotype and replication were used to determine attributes (individual berry weight, berry length, and berry width) and pyrene attributes (number/berry, dry weight/berry, and individual pyrene length, width, and height). The three-berry samples were weighed on a digital scale (Explorer, Ohause Corporation, Switzerland) and the width and height of each blackberry was measured with a certified calibrated digital caliper. Berry volume was calculated as the volume of a cone.

To determine pyrene attributes, a 0.1 mL of Pec5L enzyme (Scott Laboratories, Petaluma, CA) was added to each bag containing the three-berry frozen sample to break down the skin and pulp. Once the berries thawed, they were hand-mashed in the bags. After 1.5 hours

at 21°C, 100 mL of distilled water was added to each bag. The samples were then poured into a strainer. Under running water, the pulp was mashed against the strainer until only pyrenes remained. The pyrenes were placed onto paper towels and dried at ambient temperature (21°C) for 1.5 hours. The pyrenes for each three-berry sample were counted and weighed. The pyrenes were further dried in a laboratory oven (Fischer Scientific, Pittsburg, PA Isotemp®, Model 655F) at 55°C for approximately 24 hours. The pyrenes were removed from the oven and weighed, and then the length, width, and height of six randomly-selected individual pyrenes per genotype and replication were measured with a digital caliper. Pyrene volume was calculated as length x width x thickness. The pyrenes for each genotype and replication were placed in plastic storage bags and stored in a freezer at -20°C for further measurements. Images of the individual pyrenes were taken, after freezing, using a macro lens [Nikon D90, Tokyo, Japan; Nikon AF micro Nikkor 105mm (1:2.8 D)].

Soluble solids, pH, and titratable acidity. Three replicate three-berry samples of each cultivar and genotype were used to determine the soluble solids, pH, and titratable acidity for each genotype. Samples were thawed and placed in cheesecloth to extract the juice from the berries. Titratable acidity and pH were measured by an 877 Titrino Plus (Metrohm AG, Herisau, Switzerland) with an automated titrimeter and electrode standardized to pH 2.0, 4.0, 7.0, and 10.0 buffers. Titratable acidity was determined using 6 mL of juice diluted with 50 mL of deionized, degassed water by titration with 0.1 N sodium hydroxide (NaOH) to an endpoint of pH 8.2; results were expressed as g/L citric acid. Total soluble solids (expressed as %) was measured with a Bausch & Lomb Abbe Mark II refractometer (Scientific Instrument, Keene, NH). Soluble solids/titratable acidity ratio was calculated as soluble solids (%)/(titratable acidity (g/L)/10).

Nutraceutical Analysis

Nutraceutical analysis was conducted on each genotype in triplicate. To obtain sample extracts, samples (25 g) were homogenized with 20 mL of acetone/water/acetic (70:29.5:0.5 v/v/v) with a Euro Turrax T18 Tissuemizer (Tekmar-Dohrman Corp., Mason, OH). The samples were filtered through Miracloth (Calbiochem, La Jolla, CA), the filter cakes were isolated, and the extraction was repeated. The filtrates were adjusted to a final volume of 250 mL with extraction solvent.

High Pressure Liquid Chromatography (HPLC) analysis of ellagitannins and flavonols. Sample extracts (3 mL) were dried using a Speed Vac concentrator (ThermoSavant, Holbrook, NY) and re-suspended in 0.5 mL of extraction solvent. The reconstituted samples were passed through 0.45 μm PTFE syringe filters (Varian, Inc., Palo Alto, CA) prior to HPLC analysis. The ellagitannins were analyzed on a Waters Alliance HPLC system (Milford, MA) equipped with a Waters model 996 photodiode array detector and Millenium version 3.2 software (Waters Corp., Milford, MA). Separation was performed using a Phenomenex Aqua 5 μm C18 (250 x 4.6 mm) column (Torrance, CA) with a binary gradient of 2% acetic acid for mobile phase A and 0.5% acetic acid in water/acetonitrile (1:1 v/v) for mobile phase B at a flow rate of 1.0 mL/min. A linear gradient was run from 10 to 55% B (0-50 min), from 55 to 100% B (50-60 min), and from 100 to 10% B (60-65 min). The ellagitannins and flavonols were identified on the basis of comparison of HPLC retention times to our previous HPLC results obtained using the identical HPLC conditions and LC-MS analysis (Hager, Howard, Liyange, Lay, & Prior, 2008; Hager, Prior, & Howard, 2010). The ellagitannin peaks were quantified at 255 nm as ellagic acid equivalents using external calibration curves of ellagic acid, with results expressed as milligram ellagic acid equivalents per 100 g of fresh berry weight. The flavonols

were quantified at 360 nm as rutin with results expressed as equivalents per 100 g of fresh berry weight.

HPLC analysis of anthocyanins. Sample extracts (3 mL) were dried using a Speed Vac concentrator (ThermoSavant, Holbrook, NY) and re-suspended in 2 mL of 3% formic acid. The anthocyanin analysis by HPLC was performed based on previous methods (Cho et al., 2004; Hager, Prior, & Howard, 2008) with a 250 × 4.6 mm Symmetry C18 column (Waters Corp., Milford, MA). The mobile phase consisted of a binary gradient of 5% formic acid (A) and 100% methanol (B). The flow rate was 1.0 mL/min with a linear gradient from 2 to 60% B over 60 min. The anthocyanin peaks were quantified at 510 nm using a photodiode array detector. All anthocyanins (cyanidin 3-glucoside, cyanidin 3-rutinoside, cyanidin 3-xyloside, cyanidin 3-malonylglucoside, and cyanidin 3-dioxalylglucoside) were quantified as cyanidin 3-glucoside equivalents with total monomeric anthocyanins results expressed as milligrams per 100 g of original berry.

Total phenolics. Total phenolics were measured using the Folin-Ciocalteu assay (Slinkard & Singleton, 1977) with a gallic acid standard and a consistent standard curve based on serial dilutions. Absorbencies were measured at 760 nm, and results were expressed as gallic acid equivalents (GAE).

Oxygen Radical Absorbance Capacity (ORAC). ORAC values were determined on a dual pump BMG Fluostar Optima plate reader (Durham, NC). Results were generated by evaluating the area under the curve for test samples as compared to a Trolox standard and developing a standard curve based on dilutions (final concentrations 6.25, 12.5, 25, 50 μM) of Trolox. ORAC values were calculated using regression to TE concentration.

Design & analyses. The experiment was designed as a completely randomized design by harvest date. The composition attributes were evaluated with three replicated samples for each genotype. Analyses were conducted using JMP® (version 8.0; SAS Institute Inc., Cary, NC). Tukey's HSD (Honestly Significant Difference) was used for mean separation. Pearson's correlation was used to test the relationship between/within descriptive intensity scores and composition attributes.

Results and Discussion

The analyses of descriptive sensory attributes and the composition of blackberry genotypes from the UASDOA breeding program demonstrated significant variation among the genotypes. This information is useful for both release of cultivars and for future breeding decisions.

Descriptive Sensory Analysis

The descriptive characteristics of 20 blackberry genotypes for overall color intensity, flavor intensity, sweetness, sourness, and overall seediness varied significantly (Table 1). The visual attributes, scores for overall color intensity ranged from 6.8 (APF-156) to 8.3 (A-2316 and A-2434). The scores were highest for those genotypes that had the blackest color at evaluation; ratings were less for those that had red color on berries at evaluation.

Table 1
The scored descriptive sensory attributes (appearance, flavor, and texture) for blackberry genotypes evaluated on a 10-point scale (0=less of the attribute and 9=more of the attribute in terms of intensity), Clarksville, AR 2012.

Genotype	Overall color intensity	Overall flavor intensity	Sweetness	Sourness	Overall seediness
A-2108	7.9 abc[z]	6.4 a	5.6 ab	3.4 bcd	6.4 a
A-2215	7.9 abc	5.5 ab	6.5 a	2.5 d	4.8 a
A-2312 (Stella)	8.1 a	6.5 a	5.3 ab	3.0 cd	4.8 a
A-2316	8.3 a	5.0 ab	4.5 ab	6.0 abc	6.3 a
A-2416	7.1 abc	5.3 ab	6.1 ab	5.3 abcd	4.4 a
A-2418	7.6 abc	5.1 ab	5.4 ab	5.0 abcd	7.3 a
A-2419	7.3 abc	4.9 ab	4.1 ab	7.0 a	5.5 a
A-2434	8.3 a	5.8 ab	5.6 ab	4.4 abcd	5.9 a
A-2473	7.4 abc	5.4 ab	5.5 ab	4.0 abcd	6.3 a
APF-156	6.8 c	3.8 b	2.8 b	6.3 abc	5.8 a
APF-185	7.3 abc	5.1 ab	6.0 ab	3.5 bcd	5.9 a
APF-190	7.6 abc	4.5 ab	5.6 ab	3.3 cd	5.0 a
APF-205	6.9 bc	4.8 ab	4.3 ab	4.6 abcd	4.8 a
APF-227	7.5 abc	5.9 ab	3.8 ab	6.6 ab	5.4 a
Natchez	7.4 abc	5.1 ab	5.3 ab	4.6 abcd	6.8 a
Navaho	7.4 abc	5.1 ab	3.9 ab	5.9 abc	6.3 a
Osage	8.0 ab	4.4 ab	4.8 ab	3.9 abcd	5.0 a
Ouachita	7.6 abc	5.3 ab	4.5 ab	5.0 abcd	5.6 a
Prime-Ark® 45	7.9 abc	6.0 ab	4.8 ab	4.5 abcd	6.6 a
Tupy	7.6 abc	4.3 ab	3.5 ab	5.3 abcd	4.4 a

[z] Genotypes were evaluated in duplicate (n=2) by four trained panelists. Means with different letter(s) for each attribute are significantly different ($p < 0.05$) using Tukey's HSD.

Less variation between panelist's intensity ratings indicated that the flavor attributes for sweetness and sourness were more easily and repeatedly determined by the panelists (data not shown). In terms of flavor attributes, A-2312 ('Stella') (6.5) had the highest score for overall flavor intensity and APF-156 (3.8) the lowest score. Flavor intensity for A-2312 ('Stella') and A-2108 was scored significantly higher than APF-156 but not different among other genotypes. For the sweetness attribute, A-2215 (6.5) was scored highest and significantly different from APF-

156 (2.8), which was scored lowest. Selections A-2419 (7.0) and APF-227 (6.6) were scored highest for perceived sourness and A-2215 (2.5), A-2312 ('Stella') (3.0), and APF-190 (3.3) were scored lowest. Sourness scores for A-2419 and APF-227 were significantly higher than A-2215, A-2312 ('Stella'), and APF-190.

For the texture attributes, A-2418 (7.3), 'Natchez' (6.8), and 'Prime-Ark® 45' (6.6) had the highest scores for overall seediness (presence of seediness most notable) and 'Tupy' (4.4) and A-2416 (4.4) had the lowest. Selections APF-205, A-2312 ('Stella'), and A-2215 were scored 4.8, the second lowest. Genotypes were not significantly different for overall seediness.

Composition Analysis

Basic composition. Because flavor is affected by soluble solids content and acidity parameters (Clark et al., 2007), these factors were evaluated. Selection A-2215 (13.0%) and 'Osage' (12.4%) had the highest and APF-156 (7.8%) the lowest soluble solids content, respectively (Table 2). An ideal soluble solids content for blackberry is 10% or higher (Clark et al., 2007); it is noteworthy that only five genotypes had soluble solids contents below 10%. Juice pH ranged from 3.0 (APF-227) to 4.0 ('Osage'). Titratable acidity ranged from 4.3 g/L ('Osage') to 15.5 g/L (APF-227), a four-fold difference. Wang, Galleta, and Maas (1997) reported that a soluble solids/titratable acidity ratio of 10 was the preferred flavor experience for strawberry, and that this could be obtained with high levels of soluble solids and titratable acidity or moderate soluble solids content and low titratable acidity levels (Lewers, Wang, & Vinyard, 2010). Assuming that the findings of Wang et al. (1997) for strawberries are similar for blackberries, a soluble solids/titratable acidity ratio of 10 or greater would improve flavor perception (Lewers et al., 2010). Fourteen of the 22 genotypes evaluated had soluble solids/titratable ratios of 10 or greater. 'Osage' (30.2), A-2252 (22.9), and A-2215 (20.9) had the highest ratios and APF-156

had the lowest ratio (5.7). The measurements for soluble solids, titratable acidity and the soluble solids/titratable acidity ratios are valuable in the assessment of a selection in consideration for public release.

Table 2
Composition of blackberry genotypes, Clarksville, AR

Genotype	Soluble solids (%)	pH	Titratable acidity (g/L) [z]	Soluble solids/ titratable acidity ratio[y]
A-2108	11.4 abc[x]	3.4 bcd	8.8 abcdef	13.3 bcd
A-2215	13.0 a	3.7 ab	6.3 def	20.9 abc
A-2252	11.7 ab	3.7 abc	5.6 ef	22.9 ab
A-2312 (Stella)	11.7 ab	3.5 abcd	6.7 cdef	18.5 abcd
A-2316	9.7 abc	3.1 d	14.4 ab	6.8 d
A-2416	11.3 abc	3.2 bcd	10.8 abcdef	10.9 bcd
A-2418	9.9 abc	3.1 d	13.8 ab	7.6 d
A-2419	10.3 abc	3.2 bcd	12.3 abcde	9.2 cd
A-2434	10.8 abc	3.4 bcd	8.8 abcdef	12.7 bcd
A-2473	10.9 abc	3.4 bcd	11.5 abcde	10.5 bcd
APF-156	7.8 c	3.1 cd	13.9 ab	5.7 d
APF-185	11.4 abc	3.3 bcd	8.9 abcdef	13.0 bcd
APF-190	9.7 abc	3.6 abcd	5.9 def	17.3 abcd
APF-205	9.2 bc	3.3 bcd	10.2 abcdef	9.1 cd
APF-227	11.7 ab	3.0 d	15.5 a	7.7 d
Apache	11.7 ab	3.2 bcd	12.5 abcd	9.7 bcd
Natchez	11.1 abc	3.3 bcd	9.0 abcdef	12.5 bcd
Navaho	11.5 ab	3.2 bcd	13.2 abc	8.9 cd
Osage	12.4 ab	4.0 a	4.3 f	30.2 a
Ouachita	11.5 ab	3.3 bcd	8.7 bcdef	14.5 bcd
Prime-Ark® 45	12.0 ab	3.4 bcd	8.5 bcdef	14.3 bcd
Tupy	12.0 ab	3.4 bcd	11.3 abcde	11.1 bcd

[z] Expressed as g-equivalents of citric acid.
[y] Calculated as soluble solids content/[titratable acidity (g/L)/10].
[x] Genotypes were evaluated in triplicate (n=3). Means with different letter(s) for each attribute are significantly different ($p < 0.05$) using Tukey's HSD.

Berry attributes. The size and shape of the berries varied by genotype (Table 3). Average berry weight among genotypes varied from 5.1 g (A-2252) to 9.6 g (A-2434). Estimated berry volume ranged from 2395 mm^3 (A-2252) to 4532 mm^3 (A-2108).

Table 3
Berry and pyrene attributes of blackberry genotypes, Clarksville, AR, 2012.

Genotype	Berry weight (g)	Berry volume (mm^3)[z]	Pyrenes/ berry	Pyrene weight (mg)/berry	Pyrene weight/ berry weight (%)	Pyrene volume (mm^3)[y]
A-2108	8.6 abcd[x]	4532 a	74 defghi	324 cdef	3.8 bcdef	8.7 abcde
A-2215	7.6 abcdef	3614 abc	67 fghi	226 fgh	3.0 ef	8.1 bcdefg
A-2252	5.1 f	2395 c	61 ghi	179 gh	3.6 cdef	7.7 bcdefg
A-2312 (Stella)	8.0 abcde	3474 abc	92 cdef	330 cde	4.2 abcdef	8.9 abcd
A-2316	6.2 cdef	3066 abc	88 cdef	257 defgh	4.1 abcdef	7.0 defg
A-2416	6.5 cdef	3168 abc	73 efghi	183 gh	2.8 f	6.2 g
A-2418	7.5 abcdef	3453 abc	91 cdef	356 bcd	4.8 abc	9.4 abc
A-2419	7.8 abcdef	4027 abc	99 bcd	271 defg	3.5 cdef	6.5 fg
A-2434	9.6 a	4457 ab	110 abc	452 ab	4.7 abcd	10.7 a
A-2473	6.9 abcdef	3306 abc	94 cde	317 cdef	4.6 abcd	7.6 cdefg
APF-156	8.8 abc	4310 ab	125 a	380 bc	4.3 abcde	7.7 bcdefg
APF-185	6.8 bcdef	3532 abc	70 efghi	245 efgh	3.6 cdef	8.7 abcde
APF-190	8.5 abcd	3788 abc	84 defg	276 defg	3.3 def	8.4 bcdef
APF-205	7.7 abcdef	3635 abc	122 ab	313 cdef	4.1 abcdef	6.7 efg
APF-227	7.0 abcdef	3352 abc	91 cdef	301 cdef	4.3 abcde	8.5 bcdef
Apache	7.2 abcdef	3944 abc	74 defghi	298 cdef	4.1 abcdef	9.7 ab
Natchez	9.4 ab	4253 ab	131 a	491 a	5.2 ab	8.9 abcd
Navaho	5.3 ef	2804 bc	53 i	179 gh	3.4 cdef	8.0 bcdefg
Osage	6.9 abcdef	3725 abc	73 efghi	273 defg	4.1 abcdef	8.4 bcdef
Ouachita	6.3 cdef	3155 abc	78 defgh	259 defgh	4.1 abcdef	7.2 defg
Prime-Ark® 45	5.8 def	2768 bc	85 cdefg	318 cdef	5.4 a	8.1 bcdefg
Tupy	6.0 def	2846 abc	53 hi	160 h	2.7 f	8.1 bcdefg

[z] Volume calculated as a cone.
[y] Volume calculated as length x width x height.
[x] Genotypes were evaluated in triplicate (n=3). Means with different letter(s) for each attribute are significantly different ($p < 0.05$) using Tukey's HSD.

Pyrene attributes. 'Natchez' contained the greatest number of pyrenes (131/berry) and 'Navaho' and 'Tupy' the least (53/berry) (Table 3). Because small pyrene size (< 3 mg) is preferred in both fresh-market and processed blackberry products (Moore et al., 1975), this was assessed. Genotypes that had an individual pyrene weight of 3.0 mg or less included 'Tupy' (3.0 mg), APF-156 (3.0 mg), A-2416 (2.5 mg), APF-205 (2.6 mg), A-2252 (3.0 mg), A-2316 (2.9 mg), and A-2419 (2.7 mg). Genotypes A-2434, A-2108, and 'Apache' had individual pyrene weights of 4.0 mg or higher. Pyrene weight/berry varied from 160 mg ('Tupy') to 491 mg ('Natchez'). Darrow and Sherwood (1931) found the proportion of pyrene weight/berry weight more important than pyrene size. APF-190 had, on average, 84 pyrenes/berry, a pyrene volume of 8.4 mm^3, and a ratio of 3.3% whereas 'Prime-Ark® 45' had a significantly higher ratio of 5.4% and 85 pyrenes/berry that had an individual volume of 8.1 mm^3. Of all genotypes, 'Prime-Ark® 45' (5.4%) and 'Natchez' (5.2%) had the highest values for pyrene weight per berry to berry weight while 'Tupy' (2.7%) and A-2416 (2.8%) had the least. Even though some genotypes had a high pyrene weight per berry, these did not necessarily have the most pyrenes/berry. For example, 'Natchez', 'Prime-Ark® 45', and A-2416 had 131, 85, and 73 pyrenes/berry, respectively. Pyrene volume ranged from 6.2 mm^3 (A-2416) to 10.7 mm^3 (A-2434) (Table 3).

The images of individual pyrenes from the genotypes evaluated (Figure 1) were visually placed into three groups as classified by Wada and Reed (2010) as straight, slightly concave, and convex, based on the shape of the raphe, the lower edge of the pyrene. The following genotypes were classified as straight: A-2316, A-2418, 'Apache', APF-205, 'Osage', 'Ouachita', and 'Prime-Ark® 45'. Selections A-2416 and APF-156 were slightly concave. Selections A-2215, A-2312 ('Stella'), A-2419, A-2473, APF-185, and APF-190 were straight to slightly convex.

Selections A-2108, A-2252, A-2434, APF-227, 'Natchez', 'Navaho', and 'Tupy' were convex. Wada and colleagues (2010) found that blackberry pyrene shape and structure can be used to identify the genotype and that the pyrene shape, with respect to the lower edge, for 'Navaho' and 'Tupy' was convex. 'Natchez' was classified as straight to slightly convex and slightly convex to convex, 'Ouachita' as straight, and 'PrimeArk® 45' as straight to slightly convex (Bruce & Perkins-Veazie, 2012).

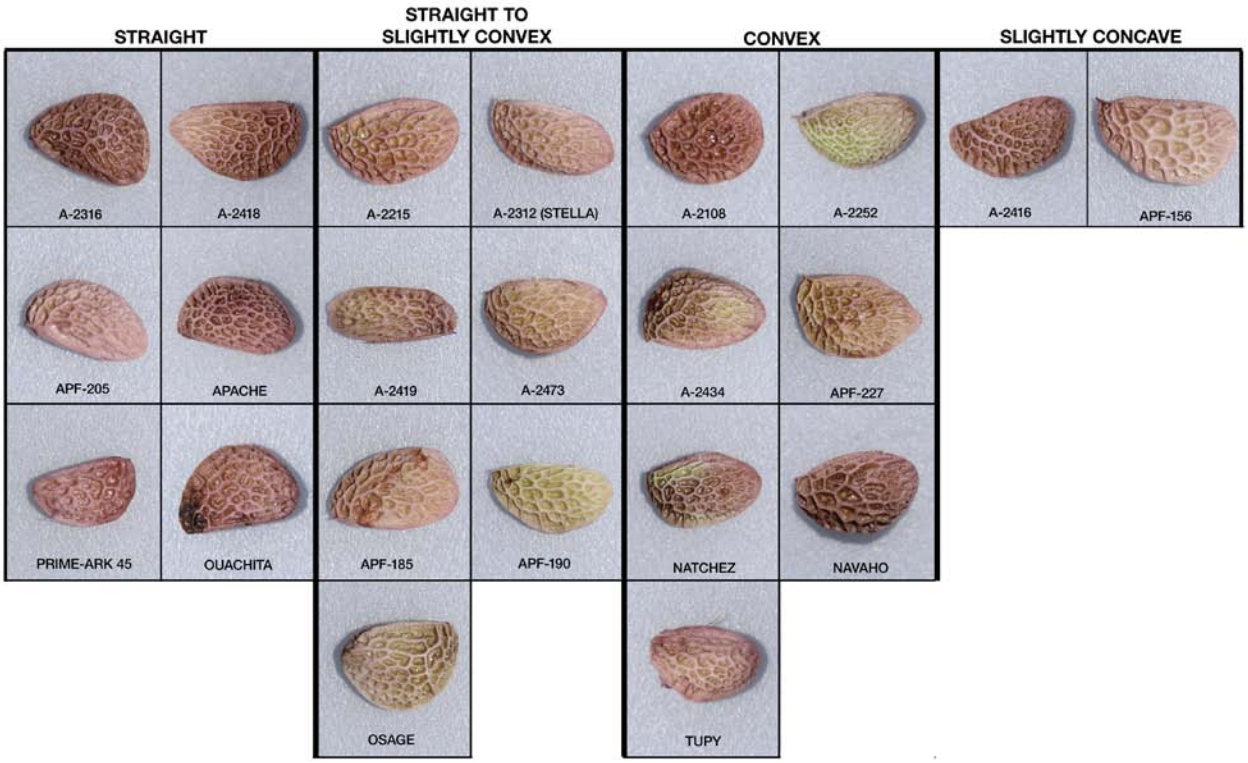

Figure 1. Images of individual pyrenes from blackberry genotypes, Clarksville, AR, 2012.
[z] Based on the shape of the raphe, the lower edge, pyrenes were visually classified into three groups: straight, slightly concave, and convex as categorized by Wada and Reed (2010). Pyrene sizes in the images are not to scale relative to each other.

Nutraceutical analysis. 'Natchez' (81.8 mg ellagic acid eqv/100 g) had the highest total ellagitannins and 'Tupy' (26.1 mg ellagic acid eqv/100 g) the lowest (Table 4). Total flavonols ranged from 9.5 mg rutin eqv/100 g ('Ouachita') to 36.8 mg rutin eqv/100 g (APF-227). Total anthocyanins ranged from 145 mg acy/100 g (A-2473) to 373 mg acy/100 g ('Apache'). Lewers

et al. (2010) reported total anthocyanins that ranged from 141 to 432 mg of cyanidin-3-glucodside eqv/100 g. Selections A-2316 (1200 mg gallic acid eqv/100 g), APF-156 (1178 mg gallic acid eqv/100 g), and 'Natchez' (1086 mg gallic acid eqv/100 g) had the highest levels of total phenolics and 'Ouachita' (515 mg gallic acid eqv/100 g) the lowest compared with values ranging from 114 to 1056 mg gallic acid eqv/100 g reported by Howard and Hager (2007). The ORAC ranged from 63.9 µmol Trolox eqv/g (APF-205) to 213.2 µmol Trolox eqv/g ('Prime-Ark® 45'). ORAC means reported by Moyer, Hummer, Finn, Frei, and Wrolstad (2002) and Lewers et al. (2010) for blackberries ranged from 13 to 146 µmol Trolox eqv/g and from 27 to 88 µmol Trolox eqv/g, respectively. 'Prime-Ark® 45' and 'Natchez' had strikingly higher ORAC values that were significantly higher than all other genotypes in this study. Among all genotypes, levels for total anthocyanins, total phenolics, total flavonols, total ellagitannins, and ORAC were among the highest for 'Natchez' compared to other tested genotypes.

Table 4
Nutraceutical attributes (based on fresh weight) for blackberry genotypes, Clarksville, AR, 2012.

Genotype	Total ellagitannins (mg ellagic acid eqv/100 g)	Total flavonols (mg rutin eqv/100 g)	Total anthocyanins (mg acy/100 g)	Total phenolics (mg gallic acid eqv/100 g)	ORAC[z] (µmol Trolox eqv/ g)
A-2108	48.4 bcdefgh[y]	15.7 efgh	343 abc	642 cdef	88.5 b
A-2215	32.9 fgh	11.9 gh	339 abc	635 cdef	83.4 b
A-2252	45.9 cdefgh	17.9 cdefgh	286 abcdef	894 abcdef	84.9 b
A-2312 (Stella)	34.1 defgh	26.3 abcde	181 fgh	662 cdef	71.0 b
A-2316	60.3 abcd	21.9 cdefg	267 abcdefgh	1200 a	90.3 b
A-2416	55.1 bcdef	20.8 cdefg	229 cdefgh	1029 abc	92.5 b
A-2418	59.6 abcde	28.2 abc	263 abcdefgh	982 abcd	102.1 b
A-2419	40.3 cdefgh	16.2 defgh	207 efgh	665 cdef	83.1 b
A-2434	52.9 bcdefg	33.5 ab	329 abcde	814 abcdef	78.4 b
A-2473	39.0 cdefgh	15.1 fgh	145 h	659 cdef	77.6 b
APF-156	38.7 cdefgh	13.5 fgh	177 fgh	1178 a	80.8 b
APF-185	38.3 cdefgh	13.5 fgh	279 abcdefg	933 abcde	92.3 b
APF-190	33.7 efgh	17.2 cdefgh	157 gh	525 ef	70.2 b
APF-205	30.0 fgh	12.6 gh	180 fgh	602 def	63.9 b
APF-227	74.7 ab	36.8 a	155 gh	839 abcdef	74.2 b
Apache	40.9 cdefgh	27.1 abcd	373 a	891 abcdef	90.6 b
Natchez	81.8 a	36.6 a	359 ab	1086 ab	202.1 a
Navaho	41.3 cdefgh	18.7 cdefgh	301 abcdef	955 abcd	82.3 b
Osage	36.4 defgh	27.8 abc	333 abcd	662 cdef	86.3 b
Ouachita	28.6 gh	9.5 h	208 defgh	515 f	70.7 b
Prime-Ark® 45	64.4 abc	24.0 bcdef	210 defgh	909 abcdef	213.2 a
Tupy	26.1 h	22.8 bcdefg	239 bcdefgh	714 bcdef	68.3 b

[z] Oxygen radical absorbance capacity=ORAC.

[y] Genotypes were evaluated in triplicate (n=3). Means with different letter(s) for each attribute are significantly different ($p < 0.05$) using Tukey's HSD.

Correlations within and between descriptive sensory analysis and composition attributes. Since there were many attributes in this study that were significantly correlated, only selected correlations are reported. Correlations are shown within each category of data (descriptive, basic composition, berry and pyrene attributes, and nutraceutical) and between data from the different categories. As expected, there are significant correlations within each

category. For all genotypes, positive and negative correlations were significant at r=0.98–0.70 (p<0.001), r= 0.69-0.56 (p<0.01), and r= 0.55-0.45 (p<0.05).

Flavor intensity was positively correlated to sweetness (r=0.47). Sweetness was negatively correlated to sourness (r=-0.74). Soluble solids content was positively correlated to pH (r=0.50) and soluble solids/titratable acidity ratio (r=0.60), but negatively correlated to titratable acidity (r=-0.46). Berry pH was positively correlated to soluble solids/titratable acidity ratio (r=0.96) and negatively correlated to titratable acidity (r=-0.91). Titratable acidity was negatively correlated to soluble solids/titratable acidity ratio (r=-0.90).

Berry weight was positively correlated to berry volume (r=0.93), pyrenes/berry (r=0.70), and pyrene weight/berry (r=0.78). Berry volume was positively correlated to pyrenes/berry (r=0.58), and pyrene weight/berry (r=0.67). Pyrenes/berry was positively correlated to pyrene weight/berry (r=0.84) and pyrene weight/berry weight ratio (r=0.63); it was negatively correlated to soluble solids (r=-0.64). Pyrene weight/berry was positively correlated to pyrene weight/berry weight ratio (r= 0.80).

Total ellagitannins was positively correlated to total flavonols (r=0.72), total phenolics (r=0.62), and ORAC (r=0.66).

For relations between descriptive and composition attributes, pyrene weight/berry was positively correlated to descriptive-evaluated overall seediness (r=0.51). Pyrene weight/berry weight ratio was also positively correlated to total ellagitannins (r=0.58), ORAC (r=0.60), and descriptive-evaluated overall seediness (r=0.70); this correlation describes the importance of pyrenes for health-promoting factors along with sensory perception of “seediness”. Berry pH was negatively correlated to total phenolics (r=-0.57) and sourness (r=-0.75). Titratable acidity was positively correlated to total phenolics (r=0.57), and sourness (r=0.82). Soluble solids

content/titratable acidity ratio was negatively correlated to total phenolics (r=-0.51) and sourness (r=-0.68), which is expected because high levels of phenolics provide a bitter taste and enhanced flavor is dependent upon low titratable acidity and perceived sourness. Total ellagitannins (r=0.57) and ORAC (r=0.54) were positively correlated to overall seediness.

Conclusion

The findings determined by this study on fresh blackberries may have the potential to provide much needed data for fruit breeders. Characteristics of fresh blackberry fruits used in this investigation varied between genotypes, some of which are likely to be improved. A finding from this study revealed that even though the sensory scores for overall seediness varied, there was a positive correlation between overall seediness and pyrene weight/berry weight ratio. The correlations within and between sensory analysis, composition attributes, and nutraceutical attributes generated by this study provide a source of information on fresh blackberries and can contribute to genotype improvement efforts at the UASDOA.

References

Bruce, M., & Perkins-Veazie, P. (2012, July). *Physical characteristics of pyrenes as a means to identify blackberry and raspberry cultivars.* Paper presented at the Annual Conference of the American Society for Horticultural Science, Miami, FL.

Cho, M. J., Howard, L. R., Prior, R. L., & Clark, J. R. (2004). Flavonoid glycosides and antioxidant capacity of various blackberry, blueberry, and red grape genotypes determined by high-performance liquid chromatography/mass spectrometry. *Journal of the Science of Food and Agriculture, 84*(13), 1771-1782. doi:10.1002/jsfa.1885

Clark, J. R. (1999). The blackberry breeding program at the University of Arkansas: Thirty-plus years of progress and developments for the future. *Acta Horticulturae, 505,* 73-77.

Clark, J. R. (2005). Changing times for eastern United States blackberries. *HortTechnology, 15*(3), 491-494.

Clark, J. R., & Finn, C. E. (2008). New trends in blackberry breeding. *Acta Horticulture, 777,* 41-47.

Clark, J. R., Howard, L. R., & Talcott, S. (2002). Antioxidant activity of blackberry genotypes. *Acta Horticulturae, 585,* 475-480.

Clark, J. R., Stafne, E. T., Hall, H. K., & Finn, C. E. (2007). Blackberry breeding and genetics. *Plant Breeding Reviews, 29,* 19-144.

Connor, A. M., Finn, C. E., & Alspach, P. A. (2005). Genotypic and environmental variation in antioxidant activity and total phenolic content among blackberry and hybridberry cultivars. *Journal of the American Society for Horticultural Science, 130*(4), 527-533.

Darrow, G. M., & Sherwood, H. (1931). Seed and berry size of cane fruits. *Proceedings of the American Society for Horticultural Science, 28*, 194-199.

Finn, C. E., & Clark, J. R. (2012). Blackberry. In: Badenes, M. L. & Byrne, D. H., (Eds.), *Handbook of Plant Breeding: Volume 8: Fruit breeding.* (pp. 151-190). New York, NY: Springer.

Hager, T. J., Howard, L. R., Liyange, R., Lay, J. O., & Prior, L. R. (2008). Ellagitannin composition of blackberry as determined by HPLCESI-MS and MALDI-TOF-MS. *Journal of Agricultural and Food Chemistry, 56*(3), 661-669. doi:10.1021/jf071990b

Hager T., Prior, R., & Howard, L. (2008). Processing and storage effects on monomeric anthocyanins, percent polymeric color, and antioxidant capacity of processed blackberry products. *Journal of Agricultural and Food Chemistry, 56*(3), 689-695. doi:10.1021/jf071994g

Hager T., Prior, R., & Howard, L. (2010). Processing and storage effects on the ellagitannin composition of processed blackberry products. *Journal of Agricultural and Food Chemistry, 58*(22), 11749-11754. doi:10.1021/jf102964b

Hall, H. K., Stephens, M. J., Stanley, C. J., Finn, C. E., & Yorgey, B. (2002). Breeding new 'Boysen' and 'Marion' cultivars. *Acta Horticulture, 585*, 91-95.

Howard, L. R., & Hager, T. J. (2007). Berry fruit phytochemicals. In Y. Zhao (ed.), *Berry fruit: Value-added products for health promotion* (pp. 73-104). Boca Raton, FL: CRC Press.

Lewers, K. S., Wang, S. Y., & Vinyard, B. T. (2010). Evaluation of blackberry cultivars and breeding selections for fruit quality traits and flowering and fruiting dates. *Crop Science, 50*(6), 2475-2491. doi:10.2135/cropsci2010.02.0097

Liu, R. H. (2003). Health benefits of fruits and vegetables are from additive and synergistic combinations of phytochemicals. *American Journal of Clinical Nutrition, 78*(3), 517S-520S.

Moore, J. N., Brown, G. R., & Brown, E. D. (1974). Relationships between fruit size and seed number and size in blackberries. *Fruit Varieties Journal, 28*, 40-50.

Moore, J. N., Lundergan, C., & Brown, E. D. (1975). Inheritance of seed size in blackberry. *Journal of the American Society for Horticultural Science, 100*(4), 377-379.

Moyer, R. A., Hummer, K. E., Finn, C. E., Frei, B., & Wrolstad, R. E. (2002). Anthocyanins, phenolics, and antioxidant capacity in diverse small fruits: *Vaccinium, rubus* and *ribes. Journal of Agricultural and Food Chemistry, 50*(3), 519-525.

Narayana, K. R., Reddy, M. S., Chaluvadi, M. R., & Krishna, D. R. (2001). Bioflavonoids classification, pharmacological, biochemical effects and therapeutic potential. *Indian Journal of Pharmacology, 33*, 2-16.

Ness, A. R., & Poulens, J. W. (1997). Fruit and vegetables, and cardiovascular disease: A review. *International Journal of Epidemiology, 26*, 1-13.

Prior, R., Cao, G., Martin, A., Sofic, E., McEwen, J., O'Brien, C., … Mainland, C. M. (1998). Antioxidant capacity as influenced by total phenolic and anthocyanin content, maturity, and variety of *Vaccinium* species. *Journal of Agricultural and Food Chemistry, 46*(7), 2686-2693.

Reyes-Carmona, J., Yousef, R. A., Martínez-Peniche, G. G., & Lila, M. A. (2005). Antioxidant capacity of fruit extracts of blackberry (*Rubus* sp.) produced in different climatic regions. *Journal of Food Science, 70*(7), 497-503. doi:10.1111/j.1365-2621.2005.tb11498.x

Sariburun E., Şahin, S., Demir, C., Türkben, C., & Uylaşer, V. (2010). Phenolic content and antioxidant activity of raspberry and blackberry cultivars. *Journal of Food Science, 75*(4), 328-335. doi:10.1111/j.1750-3841.2010.01571.x

Seeram, N. P. (2008). Berry fruits: Compositional elements, biochemical activities, and the impact of their intake on human health, performance, and disease. *Journal of Agricultural and Food Chemistry, 56*(3), 627-629.

Seeram, N. P., Adams, L. S., Zhang, Y., Lee, R., Sand, D., Scheuller, H. S., & Heber, D. (2006). Blackberry, black raspberry, blueberry, cranberry, red raspberry, and strawberry extracts inhibit growth and stimulate apoptosis of human cancer cells *in vitro. Journal of Agricultural and Food Chemistry, 54*(25), 9329-9339.

Sellappan S., Akoh, C. C., & Krewer, G. (2002). Phenolic compounds and antioxidant capacity of Georgia-grown blueberries and blackberries. *Journal of Agricultural and Food Chemistry, 50*(8), 2432-2438.

Siriwoharn, T., Wrolstad, R. E., Finn, C. E., & Pereira, C. B. (2004). Influence of cultivar, maturity, and sampling on blackberry [Rubus L. hybrids] anthocyanins, polyphenolics, and antioxidant properites. *Journal of Agricultural and Food Chemistry, 52*(26), 8021-8030.

Slinkard, K., & Singleton, V. L. (1977). Total phenol analysis: Automation and comparison with manual methods. *American Journal of Enology and Viticulture, 28*(1), 49-55.

Steinmetz, K. A., & Potter, J. D. (1996). Vegetables, fruit, and cancer prevention: A review. *Journal of the American Dietetic Association, 96*(10), 1027-2039.

Strik, B. C., Clark, J. R., Finn, C. E., & Bañados, M. P. (2007). Worldwide blackberry production. *HortTechnology, 17*(2), 205-213.

Takeda, F. (1993). Characterization of blackberry pyrenes [Abstract]. *HortScience, 28*, 488.

Tomlik-Wyremblewska, A., Zieliński, J., & Guzicka, M. (2010). Morphology and anatomy of blackberry pyrenes (*Rubus* L., Rosaceae) elementary studies of the European representatives of the genus *Rubus* L. *Flora, 205*(6), 370-375.

Van der Sluis, A. A., Dekker, M., De Jager, A., & Jongen, W. M. F. (2001). Activity and concentration of polyphenolic actioxidants in apple: Effects of cultivar, harvest year, and storage conditions. *Journal of Agricultural and Food Chemistry, 49*(8), 3606-3613.

Wada, S., Nonogaki, H., & Reed, B. M. (2010). Identifying blackberry cultivars by seed structure (#EM9002). Retrieved from Oregon State University Extension Publications Online Catalog: http://hdl.handle.net/1957/16304.

Wada, S., & Reed, B. M. (2010). Seed coat morphology differentiates blackberry cultivars. *Journal of American Pomological Society, 64*(3), 152-161.

Wang, S. Y., Galletta, G. J., & Maas, J. L. (1997). Chemical characterization of 24 strawberry cultivars and selections. *Journal of Small Fruit and Viticulture, 5*(1), 21-36. doi:10.1300/J065v05n01_02

Wang, W. D., Xu, S. Y., & Jin, M. K. (2009). Effects of different maceration enzymes on yield, clarity and anthocyanin and other polyphenol contents in blackberry juice. *International Journal of Food Science and Technology, 44*, 2342-2349. doi:10.1111/j.1365-2621.2007.01637.x

Zheng, W., & Wang, S.Y. (2003). Oxygen radical absorbing capacity of phenolics in blueberries, cranberries, chokeberries, and lingonberries. *Journal of Agricultural and Food Chemistry, 51*(2), 502-509.

EARLY INVESTIGATIONS IN CONFORMAL AND DIFFERENTIAL GEOMETRY

By Raymond T. Walter
Departments of Mathematics, Physics, and Economics

Faculty Mentor: Dr. John Ryan
Department of Mathematics

ABSTRACT

The present article introduces fundamental notions of conformal and differential geometry, especially where such notions are useful in mathematical physics applications. Its primary achievement is a nontraditional proof of the classic result of Liouville that the only conformal transformations in Euclidean space of dimension greater than two are Möbius transformations. The proof is nontraditional in the sense that it uses the standard Dirac operator on Euclidean space and is based on a representation of Möbius transformations using 2x2 matrices over a Clifford algebra. Clifford algebras and the Dirac operator are important in other applications of pure mathematics and mathematical physics, such as the Atiyah-Singer Index Theorem and the Dirac equation in relativistic quantum mechanics. Therefore, after a brief introduction, the intuitive idea of a Clifford algebra is developed. The Clifford group, or Lipschitz group, is introduced and related to representations of orthogonal transformations composed with dilations; this exhausts Section 2. Differentiation and differentiable manifolds are discussed in Section 3. In Section 4 some points of differential geometry are reiterated, the Ahlfors-Vahlen representation of Möbius transformations using 2x2 matrices over a Clifford algebra is introduced, conformal mappings are explained, and the main result is proved.

1. Introduction

The present article introduces fundamental notions of conformal and differential geometry, especially where such notions are useful in mathematical physics applications. The author considers this article as part of a broader aim of bridging the gap of understanding between mathematicians and physicists. The present article does not strongly make a connection between the mathematics presented and its applications to mathematical physics. It is instead a preliminary work, in which the mathematical tools for making such a connection are introduced with a greater emphasis on conformal than differential geometry.

The selection and treatment of topics in this article reflects the author's interest in Clifford analysis, which is the study of Clifford algebras and Dirac operators. Indeed, Section 2 begins with basic notions of Clifford algebras. Section 4 uses these notions to define a special sort of 2x2 matrices over an appropriate Clifford algebra, called Ahlfors-Vahlen matrices, that are themselves used in a proof of Liouville's classic result that the only conformal mappings on Euclidean space of dimension greater than two are Möbius transformations. In Section 3, differential geometry is developed with the eventual goal of discussing curved (Riemannian) manifolds with spin structure; on such a manifold, one can construct a Dirac operator relevant to supersymmetric quantum mechanics. The present author hopes to consider this in future work.

2. Clifford Algebras and Related Topics

1. The Clifford Algebra over $\mathbb{R}^n$

The Clifford algebra over the Euclidean space $\mathbb{R}^n$, denoted $C\ell(\mathbb{R}^n)$ or $C\ell_n$, is first constructed. Although an abstract construction is possible by factoring the tensor algebra of $\mathbb{R}^n$ by an appropriate two-sided ideal, the present construction chooses a particular basis with a particular quadratic form. Some important definitions and mappings in $C\ell_n$ are then introduced.

Porteous and Garling both provide good discussions of these notions. Garling thoroughly and formally constructs Clifford algebras over general real vector spaces.

To this end, consider $\mathbb{R}^n$ with a particular choice of basis $\{\mathbf{e_1}, \ldots, \mathbf{e_n}\}$ and the familiar dot product. Then for arbitrary vectors $\mathbf{x} = (x_1, \ldots, x_n)$ and $\mathbf{y} = (y_1, \ldots, y_n)$ in $\mathbb{R}^n$,

$$\mathbf{x} \cdot \mathbf{y} = \sum_{i=1}^{n} x_i y_i .$$

Suppose further this basis is orthonormal, so $\mathbf{e}_i \cdot \mathbf{e}_j = \delta_{ij}$ for every *i* and *j* in {1, … , *n*}. Recall the Kronecker delta δ_{ij} is 1 if *i* equals *j* and is 0 otherwise. The Clifford algebra $C\ell_n$ is defined as the span

$$< 1, \mathbf{e}_1, \ldots, \mathbf{e}_n, \ldots, \mathbf{e}_{j_1} \ldots \mathbf{e}_{j_k}, \ldots, \mathbf{e}_1 \ldots \mathbf{e}_n >, \quad 1 \le j_1 < \ldots < j_k \le n ,$$

modulo the relation $\mathbf{e}_i \mathbf{e}_j + \mathbf{e}_j \mathbf{e}_i = -2\delta_{ij}$ for every *i* and *j* in {1, … , *n*}. This condition suffices to define a multiplication on $C\ell_n$. Note that distinct indices anticommute if $n \ge 2$ and $\mathbf{e}_i^2 = -1$ for $1 \le i \le n$. By a simple combinatorial argument using the binomial theorem, dim $C\ell_n = 2^n$.

Alternatively, $C\ell_n$ is defined as the free algebra on the chosen orthonormal basis for $\mathbb{R}^n$ subject to the relation $\mathbf{e}_i \mathbf{e}_j + \mathbf{e}_j \mathbf{e}_i = -2\delta_{ij}$. The free algebra alone would be infinite-dimensional, but going modulo the relevant relation reduces the dimension to 2^n: any finite concatenation of the basis elements over the chosen basis for $\mathbb{R}^n$ is either the empty word or can be rearranged as a product $\mathbf{e}_{j_1} \ldots \mathbf{e}_{j_k}$, $1 \le j_1 < \ldots < j_k \le n$, and there are only 2^n such words (note the empty word corresponds to the identity 1).

If $\{\mathbf{e}_{j_1}, \ldots, \mathbf{e}_{j_k}\}$ has *k* elements, then the product $\mathbf{e}_{j_1} \ldots \mathbf{e}_{j_k}$ is said to be a *k*-vector, and any linear combination of such *k*-vectors is also said to be a *k*-vector. The subspace consisting of all *k*-vectors is denoted Cl_n^k, and $\mathrm{Cl}_n = \mathrm{Cl}_n^1 \oplus \ldots \oplus \mathrm{Cl}_n^n$. For $a \in \mathrm{Cl}_n$, the projection of a onto Cl_n^k is

denoted $[a]_k$. Often 0-vectors, 1-vectors, and 2-vectors are respectively referred to as scalars, vectors, and bivectors. Since $\mathbb{R}^n \cong \mathrm{Cl}^1_n \subset \mathrm{Cl}_n$, it is convenient to speak of a vector in $\mathrm{Cl}^1_n \subset \mathrm{Cl}_n$ as being a vector in $\mathbb{R}^n$. Henceforth, unless otherwise specified, each reference to a vector in $\mathbb{R}^n$ should be considered a reference to a vector in $\mathrm{Cl}^1_n \subset \mathrm{Cl}_n$ identified with a vector in $\mathbb{R}^n$. In general, for every vector $\mathbf{x} \in \mathbb{R}^n$, $\mathbf{x}^2 = -\mathbf{x} \cdot \mathbf{x}$ and orthogonal vectors anti-commute.

Throughout the present article are used three involutions on $C\ell_n$. These are mappings that, upon acting twice on an element of $C\ell_n$, return that element. Involutions on $C\ell_n$ are specified by their actions on vectors. For each $\mathbf{x} \in \mathbb{R}^n$ and a and b in $C\ell_n$, these involutions and their actions are the following.

1. The main (principal) automorphism

$$\mathbf{x}' \to -\mathbf{x},\ (ab)' = a'b' \Rightarrow (\mathbf{e}_{j_1}\ldots\mathbf{e}_{j_k})' = (-\mathbf{e}_{j_1})\ldots(-\mathbf{e}_{j_k}) = \pm\mathbf{e}_{j_1}\ldots\mathbf{e}_{j_k}$$

2. The main (principal) anti-automorphism

$$\overline{\mathbf{x}} \to -\mathbf{x}, \overline{(ab)} = \overline{b}\,\overline{a} \Rightarrow \overline{(\mathbf{e}_{j_1}\ldots\mathbf{e}_{j_k})} = (-\mathbf{e}_{j_k})\ldots(-\mathbf{e}_{j_1}) = \pm\mathbf{e}_{j_1}\ldots\mathbf{e}_{j_k}$$

3. The reversion anti-automorphism

$$\mathbf{x}^* \to \mathbf{x},\ (ab)^* = b^*a^* \Rightarrow (\mathbf{e}_{j_1}\ldots\mathbf{e}_{j_k})^* = \mathbf{e}_{j_k}\ldots\mathbf{e}_{j_i} = \pm\mathbf{e}_{j_1}\ldots\mathbf{e}_{j_k}$$

Each involution can be expressed in terms of the other two. For example, $\overline{a} = (a')^* = (a^*)'$. Since $|\mathbf{x}|^2 = \mathbf{x}\cdot\mathbf{x} = \overline{\mathbf{x}}\mathbf{x} = \mathbf{x}\overline{\mathbf{x}}$, every nonzero $\mathbf{x}$ has a well-defined multiplicative inverse $\mathbf{x}^{-1} = \overline{\mathbf{x}}/|\mathbf{x}|^2$.

2. The Lipschitz Group

The Lipschitz group over $\mathbb{R}^n$ is now introduced; it is denoted $\Gamma(n)$ and sometimes called the Clifford group. It is the subset of $C\ell_n$ generated by all invertible vectors (equivalently, all non zero vectors) in $\mathbb{R}^n$. Hence, the Lipschitz group:

$$\Gamma(n) = \{a \in C\ell_n : \exists \mathbf{x}_1, \mathbf{x}_d \in \mathbb{R}^n / \{0\}, d \in \mathbb{N} : a = x_1 \ldots x_d\}.$$

Orthogonal transformations can be represented using particular elements of the Lipschitz group. Indeed, let $\mathbf{y} \in S^{n-1} = \{\mathbf{x} \in \mathbb{R}^n : | x | = 1\}$. Consider the decomposition $\mathbf{x} = \mathbf{x}^{\parallel} + \mathbf{x}^{\perp}$, where $\mathbf{x}^{\perp}$ is a vector orthogonal to $\mathbf{y}$ (so $\mathbf{x}^{\perp}$ and $\mathbf{y}$ anticommute) and $\mathbf{x}^{\parallel}$ is a vector parallel to $\mathbf{y}$ (so $\mathbf{x}^{\parallel}$ and $\mathbf{y}$ commute). This implies $\mathbf{yxy} = \mathbf{y}(\mathbf{x}^{\parallel} + \mathbf{x}^{\perp})\mathbf{y} = -\mathbf{x}^{\parallel} + \mathbf{x}^{\perp}$, and $\mathbf{yxy}$ is a reflection of $\mathbf{x}$ in the $\mathbf{y}$-direction — say $R_{\mathbf{y}} \in O(n)$, where $O(n)$ is the orthogonal group on $\mathbb{R}^n$. Since $\mathbf{y} \in S^{n-1}$ was arbitrary, this shows there exists a reflection $R_{\mathbf{y}} \in O(n)$ for every such $\mathbf{y}$.

It is convenient to define the so-called Pin group:

$$Pin(n) = \{a \in C\ell_n : \exists \mathbf{x}_1, K, \mathbf{x}_d \in S^{n-1}, d \in \mathbb{N} : a = \mathbf{x}_1 \ldots \mathbf{x}_d\}.$$

The Pin group $Pin(n)$ is a subgroup of $\Gamma(n)$. By repeated application of the above argument for a single reflection, for $\mathbf{a} \in Pin(n)$, $\mathbf{axa}^*$ represents a (finite) sequence of reflections. By the Cartan-Dieudonne Theorem, every orthogonal transformation in $O(n)$ can be represented as such a sequence. Thus there is a surjective group homomorphism between $Pin(n)$ and $O(n)$. Note that $(-\mathbf{a})\mathbf{x}(-\mathbf{a}^*) = \mathbf{axa}^*$, so $\{\pm 1\}$ is part of (in fact, it is) the kernel of this homomorphism. This shows $Pin(n)$ is a double-cover of $O(n)$. Moreover, this shows orthogonal transformations can be represented by particular elements of the Lipschitz group.

The above arguments generalize for representing orthogonal transformations composed with dilations. Let $\beta \in \Gamma(n)$, so $\beta = (\beta/\sqrt{\beta\bar{\beta}})\sqrt{\beta\bar{\beta}} \in Pin(n) \otimes \mathbb{R}^{n}.^{+}$. Thus $\beta \mathbf{x} \beta^{*}$ represents an element of $O(n)\otimes\mathbb{R}^{n+}$. Again using the Cartan-Dieudonne Theorem, one readily shows $\Gamma(n)$ is a double cover of $O(n)\otimes\mathbb{R}^{n+}$. Hence one can represent an orthogonal transformation with a dilation using elements of the Lipschitz group. An equivalent representation is $\nu(\beta)(\mathbf{x}) = sig(\beta)\beta \mathbf{x} \bar{\beta}$, where the "sign" function is defined as $sig(\beta) = \bar{\beta}\beta' / (\beta\bar{\beta}) \in \{\pm 1\}$ and takes the value +1 or -1 in accordance with $sig(\beta)\bar{\beta} = \beta^{*}$. This equivalent representation is used by Cnops and appears below in the proof of Liouville's Theorem.

3. Differentiation on Topological Manifolds

1. Differentiation

This treatment of differentiation in several variables follows after Rudin's, by considering several cases of functions of the form $f: \Omega \to \mathbb{R}^m$ with $f: \Omega \subset \mathbb{R}^n$ an open set. It works toward the definitions stated in Aubin's treatment of differentiation. Througout the entirety of this section, the Euclidean space $\mathbb{R}^n$ (respectively, $\mathbb{R}^m$) is treated in the standard way and not identified with $Cl^{1}_{n} \subset Cl_{n}$ (respectively, $Cl^{1}_{m} \subset Cl_{m}$).

n =1 and m =1

Let f be a real-valued function with domain $(a, b) \subset \mathbb{R}$; that is, $f: (a, b) \to \mathbb{R}$. For $x_0 \in (a, b)$, the derivative of f at x_0 is the real number defined by

$$f'(x_0) = \lim_{y \to 0} \frac{f(x_0 + y) - f(x_0)}{y}, \; x_0 + y \in (a, b),$$

provided this limit exists. This implies

$$f(x_0 + y) - f(x_0) = f'(x_0)y + |y|\,\omega(x_0, y)$$

for some remainder function ω: $\mathbb{R}$ x $\mathbb{R} \to \mathbb{R}^m$ satisfying $\lim_{y \to 0} \omega(x_0, y) = 0$. This expresses the difference $f(x_0 + y) - f(x_0)$ as a linear operator mapping y to $f'(x_0)y$ plus a small remainder. Using a natural bijective correspondence that exists between $\mathbb{R}$ and $L(\mathbb{R})$, one may regard the derivative of f at x_0 as a linear operator (not a real number) that maps y to $f'(x_0)y$. [The set of all linear transformations from $\mathbb{R}^n$ to itself is denoted $L(\mathbb{R})$. More generally, for real vector spaces V and W, $L(V,W)$ is the set of all linear transformations from V and W; if $V = W$, then $L(V,W) = L(V)$. For any fixed real number, we may regard multiplication by that real number as a linear operator on $\mathbb{R}$; conversely, any linear operator from $\mathbb{R}$ to itself is multiplication by some real number.]

n =1 and m ≥1

Let f be a vector-valued function with domain $(a, b) \subset \mathbb{R}^n$; that is, $f : (a, b) \to \mathbb{R}^m$. For $x_0 \in (a, b)$, the derivative of f at x_0 is the real vector defined by

$$f'(x_0) = \lim_{y \to 0} \frac{f(x_0 + y) - f(x_0)}{y}, \; x_0 + y \in (a, b),$$

provided this limit exists. This implies

$$f(x_0 + y) - f(x_0) = f'(x_0)y + |y|\,\omega(x_0, y)$$

for some remainder functions ω: $\mathbb{R}$x$\mathbb{R} \to \mathbb{R}^m$ satisfying $\lim_{y \to 0} \omega(x_0, y) = 0$. Note that y and $(f^1(x_0)y) \in \mathbb{R}^m$, so associated with each real number y $\in \mathbb{R}$ is a real vector $(f^1(x_o)y) \in \mathbb{R}^m$. This identifies $f'(x_0)$ as a linear operator from $\mathbb{R}$ to $\mathbb{R}^m$, that is, as a member of $L(\mathbb{R}, \mathbb{R}^m)$. The only difference between the present case and the n = m = 1 case is the real number values of functions are replaced by real vector values.

Thus, for $x_0 \in (a, b) \subset \mathbb{R}$ and differentiable mapping $f: (a, b) \to \mathbb{R}^m$ with m ≥1, the

derivative of f at x_0 is the linear transformation $A \in L(\mathbb{R}, \mathbb{R}^m)$ satisfying

$$f'(x_0) = \lim_{y \to 0} \frac{|f(x_0 + y) - f(x_0) - Ay|}{|y|}.$$

n ≥1 and m ≥1

In this case, a transition is made from Rudin's treatment to Aubin's.

Definition 3.1.1. Let $\Omega \subset \mathbb{R}^n$ be an open set and let $f: \Omega \to \mathbb{R}^m$. Then f is **differentiable at** $x_0 \in \mathbb{R}^n$ if there exists a linear mapping $A \in L(\mathbb{R}^n, \mathbb{R}^m)$ such that for all $y \in \mathbb{R}^n$ satisfying $x_0 + y \in \Omega$,

$$f(x_0 + y) - f(x_0) = Ay + |y| \omega(x_0, y),$$

where $\omega \mathbb{R}^n$ x $\mathbb{R}^{n\to} \mathbb{R}^m$ is a remainder function satisfying $\lim_{y \to 0} \omega(x_0, y) = 0$. The linear mapping A is called the **differential of** f **at** x_0 and, if f is differentiable for all $x \in \Omega$, then f **is differentiable on** Ω. As A is a function of $x \in \Omega$, we may write $A = f'(x)$. If Ω Â $x \to f'(x) \in L(\mathbb{R}^n, \mathbb{R}^m)$ is a continuous map, then f is continuously differentiable on Ω $(f \in C^1(\Omega))$.[1]

The above definition raises a concern about uniqueness of the differential of f at x_0. This differential is unique: if A_1 and A_2 are both differentials of f at x_0, then one can readily show that $B = A_1 - A_2$ is identically zero.

Consider now a function (not necessarily differentiable) $f: \Omega \to \mathbb{R}^m$, where $\Omega \subset \mathbb{R}^n$ is an open set. Let $\{e_1, \mathsf{K}, e_n\}$ and $\{u_1, \mathsf{K}, u_m\}$ be standard bases of $\mathbb{R}^n$ and $\mathbb{R}^m$. The components of f are real-valued functions f_1, K, f_m such that $f(x) = \sum_{i=1}^{m} f_i(x) u_i$, for all $x \in \Omega$. For $x \in \Omega$, $1 \le i \le m$, $1 \le j \le n$, the partial derivative $D_j f_i$ is defined to be the limit

[1] Here continuity is understood in the usual sense for metric spaces (pre-images of open sets are open) and $L(\mathbb{R}^n, \mathbb{R}^m)$ is endowed with the norm defined by $||| A ||| = sup\{|Ax| : x \in \mathbb{R}^n, |x| \le 1\}$.

$$(D_j f_i)(x) = \lim_{t \to 0} \frac{f_i(x + te_j) - f_i(x)}{t},$$

provided this limit exists. This is also the derivative of f_i with respect to x_j, so $D_j f_i$ is often denoted $\frac{\partial f_i}{\partial x_j}$. If f is differentiable, then the various $D_j f_i$ exist and

$$f'(x)e_j = \sum_{i=1}^{m} (D_j f_i)(x)u_i, \ 1 \le j \le n.$$

This last expression suggests the matrix representation of $f'(x)$ with respect to the standard basis (which exists since $f'(x)$ is a linear operator), given by the $m \times n$ matrix

$$[f'(x)] = \begin{bmatrix} D_1 f_1 & \cdots & D_n f_1 \\ \vdots & \ddots & \vdots \\ D_1 f_m & \cdots & D_n f_m \end{bmatrix}.$$

In the case that $m = n$, then when f is differentiable at a point $x \in \Omega$, the Jacobian of f at x is defined as the determinant of the linear operator $f'(x)$, which may be considered as the determinant of the matrix $[f'(x)]$ in any particular basis of $\mathbb{R}^n$:

$$\frac{\partial(y_1, \ldots, y_n)}{\partial(x_1, \ldots, x_n)} = J_f(x) = \det f'(x) = \det [f'(x)].$$

It is a fact that f is C^1 on Ω if and only if all the various partial derivatives $D_j f_i$ exist and are continuous everywhere on Ω. A function f is said to be C^2 on Ω $(f \in C^2(\Omega))$ if and only if $\Omega \hat{A} x \to f'(x) \in L(\mathbb{R}^n, \mathbb{R}^m)$ is a C^1 map of Ω; more concretely, f is C^2 on Ω if and only if all the various second-order derivatives $D_i D_j f$ exist everywhere on Ω and are continuous there. Functions that are *k*-times continuously differentiable, or C^k maps ($k \in \mathbb{N}$), are defined by induction (the above function f is said to be C^3 on Ω $(f \in C^3(\Omega))$ if and only if $\Omega \hat{A} x \to f'(x)$

$\in L(\mathbb{R}^n, \mathbb{R}^m)$ is C^2 on Ω, and so on). Maps that are C^k for all $k \in \mathbb{N}$ are called C^∞ maps.

2. Manifolds and Tangent Spaces

The general notion of a topologial manifold is first introduced. The notion of local charts allows such manifolds to be treated in the familiar setting of $\mathbb{R}^n$, by mapping open neighborhoods of such manifolds to open neighborhoods of $\mathbb{R}^n$. Earlier differentiability results on $\mathbb{R}^n$ apply to these latter neighborhoods. This treatment follows after Aubin's.

Definition 3.2.1. A **manifold** M **of dimension** n is a Hausdorff topological space[2] such that each point P of M has a neighborhood Ω homeomorphic[3] to $\mathbb{R}^n$ (equivalently, to an open neighborhood of $\mathbb{R}^n$).

Definition 3.2.2. A local chart on a manifold M is a pair (Ω, φ), where Ω is an open set of M and φ a homeomorphism of Ω onto an open set of $\mathbb{R}^n$. An **atlas** is a collection of $(\Omega_i, \varphi_i)_{i \in I}$ of local charts such that $\bigcup_{i \in I} \Omega_i = M$, where I is some nonempty indexing set. The coordinates of $P \in \Omega$ related to the local chart (Ω, φ) are the coordinates of the point $\varphi(P)$ in $\mathbb{R}^n$.

Definition 3.2.3. Let $(\Omega_\alpha, \varphi_\alpha)$ and $(\Omega_\beta, \varphi_\beta)$ be local charts on M such that $\Omega_\alpha \cap \Omega_\beta \neq \varnothing$. The map $\varphi_\alpha \circ \varphi_\beta^{-1} : \varphi_\beta(\Omega_\alpha \cap \Omega_\beta) \to \varphi_\alpha(\Omega_\alpha \cap \Omega_\beta)$ is a **change of charts**. An **atlas of class** C^k (resp. C^∞) on M is an atlas for which every change of charts is C^k (resp. C^∞). This notion allows one to consider equivalence classes on C^k atlases (resp. C^∞), where two atlases $(U_i, \varphi_i)_{i \in I}$ and

[2] A topological space, in general, is a set X together with a collection of subsets T of X such that (1) $\varnothing \in T$, (2) $X \in T$, (3) T is closed under finite intersection, and (4) T is closed under arbitrary unions. The sets in T are called open sets and T is a topology on X. A topological space X is Hausdorff (also called T_2, to use the terminology of separation axioms) if, for any distinct points x and y in X, there exist disjoint open sets U and V such that $x \in U$ and $y \in V$.

[3] Two topological spaces X and Y are homeomorphic if there exists a homeomorphism $f : X \to Y$ that is a continuous bijection with a continuous inverse function.

$(W_\alpha, \Psi_\alpha)_{\alpha\in\Lambda}$ of class C^k are equivalent if their union is an atlas of class C^k (that is, $\varphi_i \circ \Psi_\alpha^{-1}$ is C^k on $\Psi_\alpha(U_i \cap W_\alpha)$ when $U_i \cap W_\alpha \neq \varnothing$). A manifold together with an equivalence class of C^k atlases is a **differentiable manifold of class** C^k.

The remainder of this discussion is restricted to a well-behaved class of manifolds, what are called paracompact manifolds.

Definition 3.2.4. A topological space X is said to **paracompact** if every open cover of X has an open refinement that is locally finite. More explicitly, for every collection of open sets $\{\Omega_i\}_{i\in I}$ (where I is a nonempty index set) such that $X \subset \bigcup_{i\in I} \Omega_i$, there exists a collection of open sets $\{\Theta_i\}_{i\in I}$ such that $\Theta_i \subset \Omega_i$ for all $i \in I$ and $X \subset \bigcup_{i\in I} \Theta_i$ (there exists an open refinement) and for every point $x \in X$ there exists a neighborhood W of x such that $\{i \in I : W \cap \Theta_i \neq \varnothing\}$ is finite (locally finite).

A related notion is a topological space that is **countable at infinity**, in which there exists a collection of compact sets $\{K_l\}_{l=1}^{\infty}$ such that $K_l \subset \operatorname{int} K_{l+1}$ for all $l \in \mathbb{N}$ and $E = \bigcup_{l=1}^{\infty} K_l$.

Theorem 3.2.5. A paracompact manifold is the union of a family of connected manifolds that are countable at infinity.

Proof This is precisely Theorem 1.1 in Aubin's book, where a proof is given.

The notion of a **partition of unity** is introduced. Let $\{\Omega_i\}_{i\in I}$ be an open cover of a topological manifold M, where I is some indexing set. A family of real-valued functions $\{\alpha_i\}_{i\in I}$ is a **partition of unity** of M if (1) any point x has a neighborhood U such that $\{i \in I : U \cap \operatorname{supp} \alpha_i \neq \varnothing\}$ is finite and (2) $0 \le \alpha_i \le 1$ (for all $i \in I$), $\sum_{i\in I} \alpha_i = 1$. This partition of

unity is **subordinate to the covering** $\{\Omega_i\}_{i\in I}$ if $\operatorname{supp}\alpha_i \subset \Omega_i$ for all $i \in I$). If each α_i is C^k, then $\{\alpha_i\}_{i\in I}$ is said to be a C^k partition of unity.

Theorem 3.2.6. On a paracompact differentiable manifold of class C^k (resp. C^∞), there exists a C^k (resp. C^∞) partition of unity subordinated to some covering.

Proof This same theorem is stated and proved as Theorem 1.12 in Aubin's book.

Definition 3.2.7. Let γ_i $(i = 1,2)$ be differentiable maps of a neighborhood of $0 \in \mathbb{R}$ into an n-dimensional manifold M such that $\gamma_i(0) = P \in M$. Let (Ω, φ) be a local chart at P. Define a relation *R* by $\gamma_1 \sim \gamma_2$ if $\varphi \circ \gamma_1$ and $\varphi \circ \gamma_2$ have the same differential at zero. The relation *R* is an equivalence relation, and a **tangent vector** X **at** P **to** M is an equivalence class for *R*.

A differentiable real-valued function f on a neighborhood of P (as in the above definition) is **flat** at P if $d(f \circ \varphi^{-1})$ is zero at $\varphi(P)$, where $d(f \circ \varphi^{-1})$ is the differential of $f \circ \varphi^{-1}$ defined on $\varphi(\Omega)$. The definition is independent of any particular chart: if Ω is as above and (Θ, ϕ) is another local chart at P, then on $\Omega \cap \Theta$,

$$d(f \circ \phi^{-1}) = d(f \circ \phi^{-1}) \circ d(\phi \circ \varphi^{-1}).$$

This allows one to introduce an alternative definition of a tangent vector, which can be shown to be equivalent to the earlier definition in terms of equivalence classes.

Definition 3.2.8. A tangent vector at $P \in M$ is a map *X*: $f \to$ X(f) $\in \mathbb{R}$ defined on the set of the differentiable functions in a neighborhood of P, where X satisfies the following two conditions:

(a) If λ and μ are real numbers, then $X(\lambda f + \mu g) = \lambda X(f) + \mu X(g)$.

(b) $X(f) = 0$ if f is flat at P.

In the above definition, conditions (a) and (b) imply that $X(fg) = f(P)X(g) + g(P)X(f)$.

This follows because

$$X(fg) = X\left(\left[(f - f(P)) + f(P)\right]\left[(g - g(P)) + g(P)\right]\right)$$

$$= X\left((f - f(P))(g - g(P))\right) + f(P)X(g) + g(P)X(f) + X\left(-2f(P)g(P)\right), \text{ the}$$

constant function $-2f(P)g(P)$ is flat for all P, and $(f - f(P))(g - g(P))$ is flat at P. [For differentiable functions h and k, $d((hk)\circ\varphi^{-1})|_{\varphi(P)} = d[(h\circ\varphi^{-1})]d[(k\circ\varphi^{-1})]|_{\varphi(P)} = 0$ if h and k are zero at P.]

Definition 3.2.9. The tangent space $T_P(M)$ at $P \in M$ is the set of tangent vectors at the point P on the n-dimensional manifold *M*.

To see that the two definitions are equivalent, one may first show that $T_P(M)$ has an n-dimensional vector space structure with the n-partial derivatives evaluated at P as a basis. This allows one to construct a bijective mapping from the equivalence classes of R (recall that these classes are families of curves) to tangent vectors in $T_P(M)$. (Aubin 45-46) A general vector space structure is evident by defining, for an arbitrary differentiable function f on *M*, addition and scalar multiplication by

$$(X + Y)(f) = X(f) + Y(f) \text{ and } (\lambda X)(f) = \lambda X(f).$$

As for dimension, let $\{x^i\}$ be the coordinate system for a local chart (Ω, φ) of *P*. Consider then the vector $(\partial/\partial x^i)_P$ in $T_P(M)$ defined by

$$\left(\frac{\partial}{\partial x^i}\right)_P (f) = \left(\frac{\partial(f\circ\varphi^{-1})}{\partial x^i}\right)_{\varphi(P)},$$

which satisfies (a) and (b) in the second definition for a tangent vector. The vectors $(\partial/\partial x^i)_P$ $(1 \le i \le n)$ are independent by the orthogonality condition $(\partial/\partial x^i)_P(x^j) = \delta_{ij}$. Moreover, these

vectors span $T_P(M)$, since $(f - \sum_{i=1}^{n} (\partial / \partial x^i)_P x^i)$ (where f differentiable) is flat, which implies

$X(f) - \sum_{i=1}^{n} (\partial / \partial x^i)_P X(x^i)) = 0$; so $X(f) = \sum_{i=1}^{n} (\partial / \partial x^i)_P X(x^i)$. It follows that $\{\partial / \partial x_P^i\}$ is a basis, and the various $X^i = X(x^i)$ are the components of $X \in T_P(M)$ in this basis. Now let $\gamma(t)$ be a map in the equivalence class $\tilde{\gamma}$ ($\gamma(0) = P \in M$) and f a real-valued function in a neighborhood of *P*. Consider the map $X : f \to [\partial(f \circ \gamma) / \partial t]_{t=0}$ (a tangent vector in the second definition). One may then define a map $\Phi : \tilde{\gamma} \to X$, since every γ_1 and γ_2 in $\tilde{\gamma}$ have the same differential at P and so $[\partial(f \circ \gamma_1) / \partial t]_{t=0} = [\partial(f \circ \gamma_2) / \partial t]_{t=0}$. It can be shown that Φ is bijective. The equivalence of the two definitions of a tangent vector follows.

The notions of smooth topological manifolds and tangent spaces at points on such manifolds are well demonstrated in classical mechanics. See the relevant discussion in the book by Takhtajan.

Definition 3.2.10. The **tangent bundle** $T(M)$ is $\bigcup_{P \in M} T_P(M)$. If $T_P^*(M)$ is the dual space of $T_P(M)$, then the **cotangent bundle** $T^*(M)$ is $\bigcup_{P \in M} T_P^*(M)$.

4. A Clifford Algebraic Approach to Möbius Transformations and Liouville's Theorem

This section introduces a Clifford algebraic approach to Möbius transformations and Liouville's Theorem. A Möbius transformation on Euclidean space is a finite composition of translations, orthogonal transformations, dilations, and inversions on that space. Such transformations are conformal; that is, they preserve measure and orientation of angles. In 1850, the French mathematician Joseph Liouville proved that, in Euclidean space of dimension greater than two, all conformal maps are Möbius transformations. In the 1930s, the Dutch mathematician

Johannes Haantjes generalized Liouville's result to nondefinite pseudo-Euclidean space (see the cited Haantjes paper). In the late 19th-century, the English geometer William Kingdon Clifford introduced what are now called Clifford algebras. In 1902, the German mathematician K.T. Vahlen introduced a representation of Möbius transformations using 2x2 matrices with entries in a Clifford algebra. This representation was largely forgotten until the late Finnish mathematician Lars Valerian Ahlfors revived it in the 1980s. The proof of Liouville's Theorem presented below uses this so-called Ahlfors-Vahlen representation, and adapts a proof by Jan Cnops. Indeed, the last two parts of this section provide a refined version of the treatment by Cnops, though restricted to the positive definite case.

1. Manifolds Revisited

The present part of Section 4 recalls the calculus on manifolds necessary to prove our main results. It also characterizes the tangent space at an arbitrary point in the Lipschitz group when considered as a manifold embedded in $C\ell_n$. General notions are discussed as in Warner's treatment rather than Aubin's. Results concerning the Lipschitz group are introduced by Cnops. Starting in Section 4.2, the remainder of this article identifies $\mathbb{R}^n$ with Cl^1_n.

Definition 4.1.1. A (smooth, parametrized) curve γ on $\mathbb{R}^n$ is an infinitely continuously differentiable (C^∞) mapping $\gamma : D \to \mathbb{R}^n$, where the domain D is an open interval of $\mathbb{R}^n$. If $0 \in D$, then γ is said to start at $\gamma(0)$ or to have a starting point at $\gamma(0)$. If $\gamma(D) \subset M$, where M is a manifold embedded in $\mathbb{R}^n$, then γ is a curve on *M*. In the present context, the tangent space $T_{\mathbf{a}}M$ at $\mathbf{a} \in M$ consists of all vectors $\mathbf{x}$ such that $\mathbf{x} = \partial_t \gamma(0)$ for some curve γ on M with starting point $\mathbf{a}$.

Definition 4.1.2. Let $f : M \to N$ be a function between two manifolds M and N embedded in $\mathbb{R}^n$. The differential of f in a point $\mathbf{a} \in M$ is the function $df_{\mathbf{a}} : T_{\mathbf{a}}M \to T_{f(\mathbf{a})}N$ such that, if the curve γ starts at $\mathbf{a}$, then $df_{\mathbf{a}}(\partial_t \gamma(0)) = \partial_t (f \circ \gamma)(0)$; note $df_{\mathbf{a}}$ is a linear map.

It is indicated without proof that $\Gamma(n)$ is a manifold embedded in $C\ell_n$. From this follows $\Gamma(n)$ is a Lie group. The tangent space of $\Gamma(n)$ at 1 is the span of Cl_n^0 and Cl_n^2 (scalars and bivectors). That is, $T_1\Gamma(n) = \mathrm{Cl}_n^0 \oplus \mathrm{Cl}_n^2$. Cnops provides a derivation of these facts (32-38). An immediate consequence is the following theorem.

Theorem 4.1.3. For arbitrary $\beta \in \Gamma(n)$, the tangent space of $\Gamma(n)$ at β is given by $T_\beta\Gamma(n) = (\mathrm{Cl}_n^0 \oplus \mathrm{Cl}_n^2)\beta = \beta(\mathrm{Cl}_n^0 \oplus \mathrm{Cl}_n^2)$.

Proof An arbitrary curve γ starting at β can be expressed in terms of a curve γ_β starting at 1, defined by $\gamma(t)\beta^{-1} = \gamma_\beta(t)$. The element $\beta \in \Gamma(n)$ is fixed, so $\partial_t \gamma(t) = \partial_t(\gamma_\beta(t))\beta$. By the preceding fact, $\partial_t \gamma(0) \in (\mathrm{Cl}_n^0 \oplus \mathrm{Cl}_n^2)\beta$. Since $\Gamma(n)$ is a manifold, $T_\beta\Gamma(n)$ has the same dimension as $T_1\Gamma(n)$. By considering an arbitrary basis of $T_1\Gamma(n)$, it follows that $T_\beta\Gamma(n) = (\mathrm{Cl}_n^0 \oplus \mathrm{Cl}_n^2)\beta$. Using $\beta^{-1}\gamma(t)$ rather than $\gamma(t)\beta^{-1}$ shows that $T_\beta\Gamma(n) = \beta(\mathrm{Cl}_n^0 \oplus \mathrm{Cl}_n^2)$, and the result follows.

2. Möbius Transformations

It turns out that, similar to the more familiar case in elementary complex analysis, Möbius transformations of $\mathbb{R}^n$ can be represented by matrices in the space of $C\ell_n$ -valued 2×2 matrices (2×2 matrices whose entries are elements of $C\ell_n$), $M(2, \mathrm{Cl}_n)$. The best geometrical motivation for the definitions in this part is given in cited paper by Ahlfors. Lounesto gives an excellent treatment of Ahlfors-Vahlen matrices in nondefinite (pseudo-Euclidean) space.

Definition 4.2.1. A matrix $A = \begin{pmatrix} a & b \\ c & d \end{pmatrix} \in M(2, \mathrm{Cl}_n)$ is an **Ahlfors-Vahlen matrix** if it fullfills the following three conditions:

(a) a, b, c, and d are products of vectors in $\mathbb{R}^n$ (equivalently, $a, b, c, d \in \Gamma(n) \cup \{0\}$)

(b) $bd^*, ac^*, a^*b, c^*d \in \mathbb{R}^n$

(c) A has nonzero real pseudodeterminant $ad^* - bc^* \in \mathbb{R}^n \{0\}$.

This may be compared to Definition 2.1 in the Ahlfors paper.

Theorem 4.2.2. Any Möbius transformation of $\mathbb{R}^n$ is given by a map $g : \mathbf{x} \to (a\mathbf{x} + b)(c\mathbf{x} + d)^{-1}$, where $A = \begin{pmatrix} a & b \\ c & d \end{pmatrix}$ is an Ahlfors-Vahlen matrix.

Proof Ahlfors states and proves an equivalent proposition as Theorem A in his paper.

The set of all Ahlfors-Vahlen matrices is a group under matrix multiplication. This indicates the representation of some classical subgroups of the group of Möbius transformations. Note that the main automorphism on $C\ell_n$ is used in representing orthogonal transformations.

$$T = \{T_{\mathbf{v}} = \begin{pmatrix} 1 & \mathbf{v} \\ 0 & 1 \end{pmatrix} : \mathbf{v} \in \mathbb{R}^n\}$$

1. Translations: ; $T_{\mathbf{u}} T_{\mathbf{v}} = T_{\mathbf{u}+\mathbf{v}}$

$$D = \{D_{\mathbf{v}} = \begin{pmatrix} \lambda & 0 \\ 0 & \lambda^{-1} \end{pmatrix} : \lambda \in \mathbb{R} / \{0\}\}$$

2. Dilations: ; $D_\lambda D_\mu = D_{\lambda\mu}$

3. Orthogonal Transformations: $R = \{R_\alpha = \begin{pmatrix} \alpha & 0 \\ 0 & \alpha' \end{pmatrix} : \alpha \in Pin(n)\}$; $R_\alpha R_\beta = R_{\alpha\beta}$

An inversion is given by any nonzero scalar multiple of $\begin{pmatrix} 0 & 1 \\ 1 & 0 \end{pmatrix}$.

3. Conformal Map

Here a conformal map is defined in Euclidean space. An expression for the differential in an arbitrary point of $\mathbb{R}^n$ is obtained, using the fact an orthogonal transformation composed with a dilation can be represented by elements of the Lipschitz group.

Definition 4.3.1. Let M and N be manifolds embedded in $\mathbb{R}^n$. Then an injective differentiable map ϕ from a domain Ω of M to a domain Π of N is said to be a conformal map if the differential $d\phi_{\mathbf{a}}$ in an arbitrary point $\mathbf{a} \in \Omega$ is, up to a nonzero factor, an isometry between the respective tangent spaces.

Any finite-dimensional real vector space is, in a natural way, a differentiable manifold, and the tangent space at any point of that space can be naturally identified with that space itself (Warner 86). Since a and $f(a)$ are in $\mathbb{R}^n$, this implies that both $T_{\mathbf{a}}\Omega$ and $T_{f(\mathbf{a})}\Pi$ are isomorphic to the real quadratic space $\mathbb{R}^n$, and $d\phi_{\mathbf{a}} : T_{\mathbf{a}}\Omega \to T_{f(\mathbf{a})}\Pi$ is an orthogonal mapping up to some nonzero factor. In the above definition of a conformal map, the relation between the respective tangent spaces becomes, for every $\mathbf{x}$ and $\mathbf{y}$ in $T_{\mathbf{a}}\Omega$,

$$\mathbf{x} \cdot \mathbf{y} = \mu(\mathbf{a})(d\phi_{\mathbf{a}}(\mathbf{x}) \cdot d\phi_{\mathbf{a}}(\mathbf{y})) = \mu(\mathbf{a})(\partial_t(\phi \circ \gamma)(0) \cdot \partial_t(\phi \circ \lambda)(0)) \quad (4.3.1)$$

where γ and λ are arbitrary curves starting at $f(a)$ for which $\mathbf{x} = \partial_t \gamma(0)$ and $\mathbf{y} = \partial_t \lambda(0)$ and $\mu(\mathbf{a})$ is some nonzero factor. The local contraction factor $\mu(\mathbf{a})$ generally depends on $\mathbf{a}$.

This characterization of conformal maps in terms of distances can be rendered in terms of angles. In Euclidean space, one may define the angle θ between two vectors $\mathbf{x}$ and $\mathbf{y}$ by $\mathbf{x} \cdot \mathbf{y} = |\mathbf{x}||\mathbf{y}|\cos\theta$, where $|\mathbf{x}| = \sqrt{\mathbf{x} \cdot \mathbf{x}}$ and $|\mathbf{y}| = \sqrt{\mathbf{y} \cdot \mathbf{y}}$. Comparing with $(4.3.1)$ above, the magnitude (not necessarily the sign) of θ is preserved.

Now recall from Section 1.2 that an orthogonal transformation composed with a dilation on $\mathbb{R}^n$ can be expressed using the Lipschitz group $\Gamma(n)$. Then, choosing a point $\mathbf{x} \in \Omega$, for some function $\beta : \Omega \to \Gamma(n)$ (a Lipschitz-valued function defined on Ω), $(4.3.1)$ becomes

$$d\phi_{\mathbf{x}} X = sig(\beta(\mathbf{x}))\beta(\mathbf{x}) X \overline{\beta(\mathbf{x})} \quad (4.3.2)$$

for the function $sig(\beta) = \overline{\beta}\beta' / (\beta\overline{\beta}) \in \{+1, -1\}$ and each X in $T_{\mathbf{x}}\Omega$.

Note that X is being acted on by a member of $O(n) \oplus \mathbb{R}^+$. Then it is not clear that β is continuous. (More explicitly, there are always at least two choices for the value of β at each $\mathbf{x} \in \Omega$. The Lipschitz group is not connected, but consists of two separated components. Conceivably, a Lipschitz-valued function could satisfy $(4.3.2)$, but for a point infinitesimally close to another point in $\mathbb{R}^n$ would be mapped to the other component of the Lipschitz group, and this Lipschitz-valued function would not be continuous. So only Lipschitz-valued functions taking values in exactly one component of $\Gamma(n)$ are considered.) Nonetheless one may choose β that is at least locally continuous. Moreover, considering a sufficiently small domain $\Omega \in \mathbb{R}^n$, one may always choose β continuous on Ω.

4. Liouville's Theorem

This final part of Section 4 develops the main results of the present article. Two lemmas are used throughout the proofs of these results.

Lemma 4.4.1. (Braid Lemma) If a vector-valued function k in three variables is symmetric in its first two variables and anti-symmetric in its last two variables, then that function is identically zero.

Proof It suffices to show that $k(x, y, z) = -k(x, y, z)$, which follows from six transpositions of the variables:

$$k(x, y, z) = -k(x, z, y) = -k(z, x, y) = k(z, y, x)$$

$$= k(y, z, x) = -k(y, x, z) = -k(x, y, z).$$

Lemma 4.4.2. Let $\mathbf{x}$ and $\mathbf{y}$ be vectors in $\mathbb{R}^n$ identfied with Cl^1_n. Then $1 + \mathbf{xy}$ is a product of vectors.

Proof If $\mathbf{x}$ or $\mathbf{y}$ is invertible (nonzero), then $1 + \mathbf{xy} = \mathbf{x}(\mathbf{x}^{-1} + \mathbf{y})$ or $1 + \mathbf{xy} = (\mathbf{y}^{-1} + \mathbf{x})\mathbf{y}$. If $\mathbf{x}$ or $\mathbf{y}$ is zero, then $1 + \mathbf{xy} = 1$, which is the product of any invertible vector with its inverse.

The following discussion determines for a continuously differentiable Lipschitz-valued function $\beta : \Omega \to \Gamma(n)$ sufficient conditions for the existence of a conformal map ϕ whose differential satisfies $(4.3.2)$. The notation $\beta^{-1}(\mathbf{x})$ is used for $1/\beta(\mathbf{x})$. Also used is the Dirac operator on $\mathbb{R}^n$ applied to a scalar function, say *f*, which coincides with the familiar gradient operator: $D_X f(\mathbf{x}) = -X \cdot Df(\mathbf{x})$. In an orthonormal basis $\{\mathbf{e}_1, \ldots, \mathbf{e}_n\}$ of $\mathbb{R}^n$, $D = \sum_{k=1}^{n} \mathbf{e}_k (\partial / \partial x_k)$.

Theorem 4.4.3. Let Ω and Π be domains in $\mathbb{R}^n$. Suppose $\beta : \Omega \to \Gamma(n)$ is a continuously differentiable Lipschitz-valued function. Then there exists a conformal map $\phi : \Omega \to \Pi$ such that, for all $\mathbf{x} \in \mathbb{R}^n$,

$$d\phi_{\mathbf{x}} X = sig(\beta(\mathbf{x}))\beta(\mathbf{x}) X \overline{\beta(\mathbf{x})}, \; sig(\beta) = \overline{\beta}\beta' / (\beta\overline{\beta}) \in \{+1, -1\}, \; \forall X \in T_{\mathbf{x}}\Omega \quad (4.4.1)$$

only if there exists a vector-valued function $\mathbf{v}$: $\Omega \to \mathbb{R}^n$ such that

$$(D_X \beta^{-1}(\mathbf{x}))\beta(\mathbf{x}) = X\mathbf{v}(\mathbf{x}), \; \mathbf{v} = \frac{1}{2} D(\beta\overline{\beta}) / (\beta\overline{\beta}) \quad (4.4.2).$$

Proof It is convenient to adopt a standard orthogonal basis $\{\mathbf{e}_1, \ldots, \mathbf{e}_n\}$. By linearity, if the result holds for each $\mathbf{e}_i$ $(1 \le i \le n)$, then it holds for all $X \in T_{\mathrm{x}}\Omega = \mathbb{R}^n$. Choose such i. By the earlier result concerning the tangent space at an arbitrary point in $\Gamma(n)$, $\partial_i \beta^{-1} = B_i \beta^{-1}$ for some

$B_i \in \mathrm{Cl}^0_n \oplus \mathrm{Cl}^2_n$. Using $\beta\beta^{-1} = 1$, $\partial_i(\beta\beta^{-1}) = 0$. By the product rule, $B_i = (\partial_i \beta^{-1})\beta = -\beta^{-1}(\partial_i \beta)$.

By explicit calculation from the definition of the differential of a differentiable function ϕ for $X = \mathbf{e}_i$ and supposing $(4.4.1)$ holds, it follows $\partial_i \phi = sig(\beta)\beta \mathbf{e}_i \overline{\beta}$. As β is continuously differentiable, $\partial_j \partial_i \phi$ exists and is continuous. As i and j are arbitrary, this implies the integrability condition ϕ given by $\partial_i \partial_j \phi = \partial_j \partial_i \phi$ for arbitrary indices i and j. If ϕ has a differential of the form appearing in $(4.4.1)$, then the integrability condition becomes,

$$\partial_j (sig(\beta)\beta \mathbf{e}_i \overline{\beta}) = \partial_i (sig(\beta)\beta \mathbf{e}_j \overline{\beta}) \quad (4.4.3).$$

The function $sig(\beta) \in \{+1, -1\}$ is also continuously differentiable since β and $\overline{\beta}$ are, so any partial derivatives of $sig(\beta)$ for given $\mathbf{x} \in \Omega$ must be zero. Then $sig(\beta)$ drops out. Together with the product rule, this implies

$$(\partial_j \beta)\mathbf{e}_i \overline{\beta} + \beta \mathbf{e}_i (\partial_j \overline{\beta}) = (\partial_i \beta)\mathbf{e}_j \overline{\beta} + \beta \mathbf{e}_j (\partial_i \overline{\beta}) \quad (4.4.4).$$

Multiplying by $-\beta^{-1}$ on the left and $\overline{\beta}^{-1}$ on the right,

$$-\beta^{-1}(\partial_j \beta)\mathbf{e}_i - \mathbf{e}_i (\partial_j \overline{\beta})\overline{\beta}^{-1} = -\beta^{-1}(\partial_i \beta)\mathbf{e}_j - \mathbf{e}_j (\partial_i \overline{\beta})\overline{\beta}^{-1} \quad (4.4.5).$$

Using $\overline{\beta}^{-1} = \beta / (\beta\overline{\beta}) = \overline{\overline{\beta} / (\beta\overline{\beta})} = \overline{\beta^{-1}}$ and $\overline{\partial_i \beta} = \partial_i \overline{\beta}$, this gives $\overline{B_i} = \overline{-\beta^{-1}(\partial_i \beta)} = -(\partial_i \overline{\beta})\overline{\beta^{-1}}$. Substituting this into $(4.4.5)$,

$$B_j \mathbf{e}_i + \mathbf{e}_i \overline{B_j} = B_i \mathbf{e}_j + \mathbf{e}_j \overline{B_i} \quad (4.4.6).$$

As $B_i \in \mathrm{Cl}^0_n \oplus \mathrm{Cl}^2_n$, one may decompose B_i into its scalar and bivector parts

$$B_i = [B_k]_0 + \sum_{j,k,j\neq k} T^i_{jk} \mathbf{e}_j \mathbf{e}_k = \sum_{j,k} T^i_{jk} \mathbf{e}_j \mathbf{e}_k \text{ and } \overline{B_i} = [B_k]_0 - \sum_{j,k,j\neq k} T^i_{jk} \mathbf{e}_j \mathbf{e}_k = \sum_{j,k} T^i_{jk} \mathbf{e}_k \mathbf{e}_j \quad (4.4.7),$$

where $T^i_{jk} = -T^i_{kj}$, $j \neq k$, and $T^i_{kk} = \frac{1}{2}(-\mathbf{e}_k^2)[B_i]_0$. This used $\mathbf{e}_k^4 = (\mathbf{e}_k^2)^2 = 1$ (equivalently, $\mathbf{e}_k^2 = \mathbf{e}_k^{-2}$)

and the anti-commutativity of all distinct $\mathbf{e}_j$ and $\mathbf{e}_k$ in a standard orthogonal basis. Using $(4.4.7)$, $(4.4.6)$ may be written as

$$4(-\mathbf{e}_i^2)\sum_k T_{ik}^{\ j}\mathbf{e}_k = 4(-\mathbf{e}_j^2)\sum_k T_{jk}^{\ i}\mathbf{e}_k \quad (4.4.8).$$

For distinct i, j, and k (if $n \le 2$, then one may proceed to the case of at least two equal indices), $T_{jk}^{\ i}$ has been defined as anti-symmetric in its lower two indices. Using $\mathbf{e}_i^2 = \mathbf{e}_j^2 = -1$ and considering $(4.4.8)$ component-wise, one sees $T_{ik}^{\ j}$ is symmetric in the upper and lower left indices. By the Braid Lemma, such $T_{ik}^{\ j}$ is identically zero. Then the only remaining terms in B_i and $(4.4.8)$ (considered component-wise) include at least two equal indices: $B_i = -2\mathbf{e}_i\sum_k T_{ki}^{\ i}\mathbf{e}_k$ and $\mathbf{e}_k^2 T_{ki}^{\ i} = \mathbf{e}_i^2 T_{ii}^{\ k}$. Hence

$$B_i = -2\mathbf{e}_i(\sum_k T_{ki}^{\ i}\mathbf{e}_k) = -2\mathbf{e}_i(\sum_k (\mathbf{e}_i^2 T_{ii}^{\ k}\mathbf{e}_k^2)\mathbf{e}_k = -2\mathbf{e}_i(\sum_k (\mathbf{e}_i^2(\frac{1}{2}(-\mathbf{e}_i^2)[B_k]_0)\mathbf{e}_k^2)\mathbf{e}_k$$

$$= \mathbf{e}_i(\sum_k (\mathbf{e}_i^4[B_k]_0\mathbf{e}_k^3) = \mathbf{e}_i(\sum_k [B_k]_0\mathbf{e}_k^{-1})$$

To complete the proof, it suffices to show that $[B_k]_0 = -\frac{1}{2}\partial_k(\beta\overline{\beta})/(\beta\overline{\beta})$, from which it will follow that $B_i = (\partial_k\beta^{-1}(\mathbf{x}))\beta(\mathbf{x}) = -\mathbf{e}_i\sum_k (\partial_k(\beta\overline{\beta})/(\beta\overline{\beta}))\mathbf{e}_k^{-1} = \mathbf{e}_i D(\beta\overline{\beta})/(\beta\overline{\beta}) = \mathbf{e}_i\mathbf{v}$, where $\mathbf{v}$ has the same meaning as in the statement of the theorem. This is straightforward:

$$\partial_k(\beta\overline{\beta}) = (\partial_k\beta)\overline{\beta} + \beta(\partial_k\overline{\beta}) = -\beta B_k\overline{\beta} - \beta\overline{B_k}\overline{\beta} = -2\beta(B_k + \overline{B_k})\overline{\beta} = -2\beta[B_k]_0\overline{\beta}.$$

The above used $B_k = -\beta^{-1}(\partial_k\beta)$ implies $-\beta B_k = (\partial_k\beta)$ implies $-\overline{\beta B_k} = \partial_k\overline{\beta}$, and the earlier expressions $B_i = [B_k]_0 + \sum_{j,k,j\neq k} T_{jk}^{\ i}\mathbf{e}_j\mathbf{e}_k =$ and $\overline{B_i} = [B_k]_0 - \sum_{j,k,j\neq k} T_{jk}^{\ i}\mathbf{e}_j\mathbf{e}_k$.

For Euclidean space of dimension greater than two, there is a rather restrictive condition that β^{-1} is linear in $\mathbf{x} \in \mathbb{R}^n$ if $(4.4.1)$ in the statement of the previous theorem holds.

Corollary 4.4.4. Suppose that the hypotheses of the preceding theorem hold. Suppose further $n > 2$ and ϕ is three times continuously differentiable. Then β^{-1} has the form $\mathbf{x}\gamma + \delta$, where γ and δ are constants in the Lipschitz group.

Proof Since ϕ is at least three times continuously differentiable, using $(4.4.1)$ gives β is at least two times continuously differentiable. Noting that $\partial_k \beta^{-1} = -\beta^{-1}(\partial_k \beta)\beta^{-1}$, it is also true β^{-1} is at least two times continuously differentiable. By Theorem 4.4.3, $\partial_k \beta^{-1}(\mathbf{x}) = \mathbf{e}_k(\mathbf{v}(\mathbf{x})\beta^{-1}(\mathbf{x}))$. This determines β^{-1} up to an additive constant (say δ).

Taking second derivatives, which are symmetric in arbitrary indices ($\partial_j \partial_k \beta^{-1} = \partial_k \partial_j \beta^{-1}$ for all j and k), $\mathbf{e}_j \partial_k(\mathbf{v}(\mathbf{x})\beta^{-1}) = \mathbf{e}_k \partial_j(\mathbf{v}(\mathbf{x})\beta^{-1})$.

Distinct indices anti-commute in the chosen basis, so $\mathbf{e}_i\mathbf{e}_j \partial_k(\mathbf{v}(\mathbf{x})\beta^{-1}) = \mathbf{e}_i\mathbf{e}_k \partial_j(\mathbf{v}(\mathbf{x})\beta^{-1})$ is anti-symmetric in its first two indices ($j \neq i \neq k$) and symmetric in the last two indices . By the Braid Lemma, $\mathbf{e}_i\mathbf{e}_j \partial_k(\mathbf{v}(\mathbf{x})\beta^{-1})$ is identically zero. Multiplying $\mathbf{e}_i\mathbf{e}_j \partial_k(\mathbf{v}(\mathbf{x})\beta^{-1})$ on the left by $\mathbf{e}_j^{-1}\mathbf{e}_i^{-1}$ gives $\partial_k(\mathbf{v}(\mathbf{x})\beta^{-1}) = 0$. Then $\mathbf{v}(\mathbf{x})\beta^{-1}(\mathbf{x})$ is a constant; call it γ.

Now to state and prove Liouville's Theorem.

Theorem 4.4.5 (Liouville's Theorem) Under the conditions of the preceding theorem and corollary, ϕ is a Möbius transformation.

Proof Our goal is to find a Möbius transformation that is equivalent to ϕ and represented by an Ahlfors-Vahlen matrix $A = \begin{pmatrix} a & b \\ c & d \end{pmatrix}$. Note that a Möbius transformation

$g : \mathbf{x} \to (a\mathbf{x} + b)(c\mathbf{x} + d)^{-1}$ in the point $\mathbf{x} = 0$ is particularly simple: $g(0) = bd^{-1}$. Suppose then, to simplify matters, that $0 \in \Omega$ (if $0 \notin \Omega$, then a translation must be included first). Suppose further that $\beta(0) = 1$ (if $\beta(0) \neq 1$, then consider $\phi \circ \nu(\beta^{-1}(0))$ defined on $\nu(\beta(0))(\Omega)$, which is equivalent to ϕ on Ω. This reduces to $\beta(0) = 1$, except that one must include an orthogonal transformation first.)

Choose $b = g(0)$ and $d = 1$. The pseudo-determinant $ad^* - bc^*$ is only determined up to a multiplicative nonzero scalar (constant), so one may choose $ad^* - bc^* = 1$ and therefore $a = 1 + bc^*$. By Lemma 4.4.2, a is the product of vectors if c is a vector. The coefficient c is determined by the differential of ϕ, to which the differential of g must be equal. This differential condition is

$$dg_{\mathbf{x}}X = (ad^* - bc^*)(c\mathbf{x} + d)^{*-1}X(c\mathbf{x} + d)^{-1} = (c\mathbf{x} + 1)^{*-1}X(c\mathbf{x} + 1)^{-1}$$

$$= sig(\beta(\mathbf{x}))\beta(\mathbf{x})X\overline{\beta(\mathbf{x})} = d\phi_{\mathbf{x}}X = \beta(\mathbf{x})X(\beta(\mathbf{x}))^*,$$

where in the last line was used $(\beta(\mathbf{x}))^* = sig(\beta(\mathbf{x}))\overline{\beta(\mathbf{x})}$, which holds at $\mathbf{x} = 0$ (by the choice of $\beta(0)$, $(\beta(0))^* = 1$; the image of $\beta(0)$ under the main and reversion anti-automorphisms is also 1) and throughout Ω (by the continuity of β and its anti-automorphisms, together with the constancy of $sig(\beta)$ established in an earlier argument). By Corollary 4.4.4, $\beta^{-1}(\mathbf{x}) = \mathbf{x}\gamma + \delta$ for Lipschitz-valued constants γ and δ. If one lets $c = \gamma = \mathbf{v}(\mathbf{x})\beta^{-1}(\mathbf{x}) = \frac{1}{2}(D(\beta\overline{\beta})/(\beta\overline{\beta}))\beta^{-1}$ and $d = \delta = 1$, the equality above follows readily using $(a^*)^{-1} = (a^{-1})^*$ for $a \in C\ell_n$. Using $\beta(0) = 1$, it follows that c is a vector.

Thus has been found a matrix A whose entries satisfy conditions (a) and (c) for the above definition of an Ahlfors-Vahlen matrix. It remains to show that condition (b) is satisfied. Since b and c are vectors and $d = 1$, $bd^* = b$ and $c^*d = c^*$ are also vectors. Also since b and c are vectors, b^*b and c^*c^* are real. Then $ac^* = (1 + bc^*)c^* = c^* + b(c^*c^*)$ and $a^*b = (1 + cb^*)b = b + c^*(b^*b)$ are vectors. Hence condition (b) of the above for an Ahlfors-Vahlen matrix is satisfied. So ϕ is a Möbius transformation.

It is useful to recapitulate the main result with all hypotheses stated.

Theorem 4.4.5 (Liouville's Theorem Restated) Let Ω and Π be domains in $\mathbb{R}^n$ with $n > 2$. Then every conformal map $\phi : \Omega \to \Pi$ that is at least three times continuously differentiable is a Möbius transformation. Moreover, this Möbius transformation can be represented by an Ahlfors-Vahlen matrix.

Works Cited

Ahlfors, Lars V. "Möbius Transformations and Clifford Numbers." *Differential Geometry and Complex Analysis*. Berlin, Heidelberg: Springer-Verlag, 1985. Print.

Aubin, Thierry. *A Course in Differential Geometry*. Providence, RI: American Mathematical Society, 2001. Graduate Studies in Mathematics Vol. 27. Print.

Cnops, Jan. *An Introduction to Dirac Operators on Manifolds*. Boston: Birkhäuser, 2002. Print. Progress in Mathematical Physics Vol. 24. Garling, D. J. H. *Clifford Algebras: An Introduction*. Cambridge: Cambridge UP, 2011. Print. London Mathematical Society Student Texts Vol. 78.

Haantjes, J. "Conformal representations of an n-dimensional euclidean space with a non-definite fundamental form on itself." *Proc. Kon. Nederl. Akad. Amsterdam* 40 (1937): 700-705.

Liouville, Joseph. "Extension Au Cas Des Trois Dimensions De La Question Du Tracé Géographique." *Applications de l'analyse à la Géométrie*. Ed. Gaspard Monge. Paris: Bachelie, 1850. 609-17.

Lounesto, Pertti. *Clifford Algebras and Spinors*. 2nd ed. Cambridge: Cambridge UP, 2001. Print. London Mathematical Society Lecture Note Ser. 78.

Porteous, Ian R. *Clifford Algebras and the Classical Groups*. Cambridge: Cambridge UP, 1995. Print. Cambridge Studies in Advanced Mathematics Vol. 50.

Rudin, Walter. *Principles of Mathematical Analysis*. 3rd ed. New York: McGraw, 1976. Print.

Takhtajan, Leon A. *Quantum Mechanics for Mathematicians*. Providence, RI: American Mathematical Society, 2008. Print. Graduate Studies in Mathematics Vol. 95.

Warner, Frank W. *Foundations of Differentiable Manifolds and Lie Groups*. New York: Springer, 1983. Print. Graduate Texts in Mathematics Vol. 94.

CLASS STATUS AND IDENTITY: A SEMANTIC READING OF THE TYPICAL TRINIDADIAN HOUSE

By Leniqueca Welcome
Fay Jones School of Architecture

Faculty Mentor: Greg Herman
Fay Jones School of Architecture

Abstract

This manuscript analyzes the use of ornamentation on the exterior of residential architecture, in early 20th century Trinidad, as a hybridized product of a class system developed during Colonialism. The manuscript begins with the examination of the socio-political context of late 18th, 19th and early 20th century Trinidadian society, looking specifically at how a boom in the cocoa industry in the 1870's allowed social mobility for free coloreds and blacks. As a result, this nouveau bourgeois class of cocoa planters sought to affirm their status by displaying their identity in the strongly European influenced houses they designed. The architectural details and ornamentation of the Boissière House will be discussed in depth as a representative example of these nouveau bourgeois mansions. In conclusion, the paper will demonstrate the architectural influence of the elite on other aspiring classes.

Opulence in the Era of Cocoa

In the northwest of Port-of–Spain, Trinidad, around the Queen's Park Savannah, are located some of the island's most magnificent and ostentatious mansions. These early 20th century houses are exemplars of the peak of aristocracy in Trinidad. Each mansion draws from European precedents, combining them in distinctly different ways to create an artifact that is an expression of the identity of its commissioner. The most unique of these houses, carrying the greatest signature of owner, is the Boissière House. The Boissière House stands as a physical manifestation of the elevated class position of French creole free coloreds at the turn of the 20th century, after years of subjugation. It is important to note that the term "free coloreds" is typically used in Trinidad to define a group of individuals of white and African lineage; the term is not considered outdated or derogatory in Trinidad as it might be viewed in the United States.

Arrival of the French

In 1498, during his third voyage to the Lesser Antilles, Christopher Columbus and his crew sighted and landed on the island of Trinidad and declared it a Spanish territory. Trinidad, in its early years under Spanish rule, remained underdeveloped because there was no established plantation economy and the population remained sparse. The Spanish government, in recognition of the precarious state of the colony, introduced the 1783 *Cedula of Population*, whereby the island was opened to immigration, in an attempt to attract wealthy, white, French planters. The *Cedula* was successful as an influx of white French planters soon arrived, along with their slave labor (Brereton, 1981). French immigrants comprised the largest group of land-owners and slave holders; they also had the largest accumulation of capital and subsequently superseded the Spaniards to achieve the pinnacle of the social hierarchy.

Although the *Cedula* was important for the introduction of various European groups into Trinidad, it was more revolutionary for the rights given to the free blacks and free coloreds. For example, articles four and five of the Cedula offered land grants and civil rights to free coloreds and free blacks who were planters and slave holders. Free coloreds and blacks were granted 15 acres of land for each member of his family and half as much for each slave he introduced (Brereton, 1981). Concurrent to the issuing of this decree, free coloreds were severely mistreated in the British and French territories of the Caribbean. In these islands, a system of apartheid was reaching its climax; free coloreds and blacks were subject to increasingly severe restrictions on economic activity and humiliating regulations. No matter how educated or wealthy they were, the legislation enforced in the British and French territories ensured that free coloreds were treated and perceived as inferior to whites. Considering the time period and social condition of free coloreds and free blacks on the other islands, the peculiarity of this decree is undeniable. Not only did the decree promote the influx of free coloreds and free blacks to Trinidad, but it also promised increased economic security and elevated social status. By 1797, the free colored and free black population in Trinidad totaled 4,476; it almost doubled the white population of 2,151 members (Brereton, 1981).

In 1784, Don Jose Maria Chacon arrived in Trinidad to assume his place as the Spanish governor of the island. Chacon was described as well-educated, enlightened, reform-minded, fluent in French and English and sympathetic to French immigrants (Brereton, 1981). Spanish colonies were already well-known for having a more lenient view on harsh laws against free coloreds, however Chacon was even more liberal in his treatment. For instance, Chacon chose to ignore laws crafted against the coloreds and spared them from any public humiliation or

marginalization. He also appointed free coloreds and free black land-owners to officers' commissions in the militia.

The milder working conditions offered to free blacks and coloreds were powerful because of the psychological effect it had on this group, especially with regard to the free coloreds. The free coloreds consisted of a social group in which the members, despite being theoretically "free", had white lineage and aligned themselves with white European culture; however they were still considered inferior by the larger society because of their African lineage. As such, they were accustomed to being dominated and dehumanized with no apparent escape from the situation. Neither education nor the accumulation of assets could alter the opinion of white planters in British and French colonies where free coloreds resided. However, after relocating to Trinidad, free coloreds were immersed in a social climate where they were granted rights and were treated with courtesy and dignity. In this new society, they could gain social standing if they became prosperous. This improved condition was symbolically important to the free coloreds who formed a powerful upper-middle income group with the promise of growing more successful and more influential in society.

The Oppression of French, Free Coloreds

With the change in Trinidad's political climate, the French colored planters were not as fortunate as the white French planters in maintaining their rank in society; as a result, they met an unfortunate fate. After the capture of Trinidad by the British, the privileged position that the free coloreds enjoyed under Chacon soon dissipated. Sir Ralph Abercromby, who captured Trinidad for Britain in 1797, named Thomas Picton, an officer on his staff, the military governor and commander-in-chief of the island. Abusing his power, Picton was given free reign to instate a regime of tyranny and terror in Trinidad. The worst treatment was inflicted on the slaves and

the free coloreds. Picton perpetuated the stereotype that the French free coloreds were dangerous revolutionaries and used this to justify his atrocities against them. He referred to them as "a dangerous class which must gradually be got rid of" (Brereton, 1981). Picton also subjected free coloreds to legal discrimination and social humiliation by torturing, imprisoning, and executing coloreds without reason or trial. Picton's actions were deemed harsh even by 19th century, British Imperial standards and he later became the subject of British indictment.

William Fullerton, a commissioner sent to Trinidad by the British government to investigate Picton, was shocked by the treatment of slaves and free coloreds. As a result, he launched a campaign against Picton. Fullerton lobbied for a fair judicial process when prosecuting slaves and free coloreds, but he was perceived by the white elite as liberal and undermining the established system of order. Whites who aligned with Picton's regime feared that if they gave coloreds even the most minimal rights it would thwart the structure of racial supremacy. A French white planter summed up the feelings of the general white population toward Fullerton's compassion for coloreds when he complained that Fullerton's actions would "undermine the basis of the colonial system of Government in a country where the Colored People are numerous and the least relaxation of subordination would produce the most serious consequences" (Brereton,1981, p. 40). The climate of the colony had changed in terms of how the free colored community was treated. All coloreds, no matter their rank or education, were treated with contempt, causing a crippling setback to the entire group. Gone were the days of empowerment where they had the ability to ascend the ranks to be perceived as a meaningful, respectable class in society. This reprehensible and oppressive situation would not change until the post-emancipation period.

The Renaissance of the French Free Coloreds

The momentous end of the slave system in Trinidad also marked an important milestone for the island - the beginning of a formal economy for Trinidad. Two events marked this formal economy, the establishment of paid labor and the Colonial Bank. With the acquisition of wages, blacks now had money to invest; many invested their acquired capital in the newly developing cocoa economy.

A sugar economy was non-existent in Trinidad under the Spanish rule. While the French introduced the sugar industry, it did not flourish until the arrival of the British. The sugarcane economy remained an exclusive, rich, British, white man's market. The sugarcane estates that were established by the French colored planters before British capitalization of the market gradually died out as British planters bought them. British colonialists were not concerned with the cocoa industry; as a result, it provided an opportunity for both white and colored French Creoles to dominate the market. They became the capitalists for the cocoa industry, benefiting from the investments and production of the former slaves. French coloreds used the cocoa economy to form an aristocratic upper middle-class after their years of subjugation.

Undoubtedly, the quality of Trinidad's cocoa is one of the richest found in the world and contributed to the economic development of the nation. There had always been small cocoa farmers in Trinidad, usually of French or Spanish descent, but before the 1860s, they did not have a substantial market for the cocoa in either Spain or Britain. Thus, there was no formal cocoa economy on the island. However, following technological advances in cocoa processing in the 1860s, the cocoa drink became an item of mass consumption in Europe and the United States. In 1866, the Cadbury Company began producing solid chocolates in Britain (Brereton, 1981). This tremendous expansion in the British market led to a boom in cocoa production in Trinidad.

Additionally, the extension of roads, development of railways, and launch of undeveloped Crown lands for sale also helped boost cocoa production. A depression in the sugar industry after 1884 allowed for the release of labor, capital, and land that could be used towards the production of cocoa. Hence, the cocoa industry enjoyed a significant expansion from 1866-1920, thereby surpassing sugar as the island's leading export.

The trickle down structure of the cocoa industry provided opportunities for various different social groups. Though the industry was controlled by French creole whites and coloreds, the Trinidad cocoa industry was pioneered and developed by peasants. At the time of emancipation there were millions of acres of Crown lands that were uncultivated or under-cultivated, and this land was used to develop the cocoa industry. There were two ways in which these cocoa estates were established. The first method for the establishment of a cocoa plantation entailed a peasant, usually an ex-slave, buying a small portion of Crown lands with his labor wages. The peasant then cleared the land and planted cocoa trees on it. After the trees began to bear, the peasant sold the bearing trees and the land to a cocoa planter, usually a French creole, who then turned the already producing land into a large estate. The peasants then used the proceeds to buy another area of land and repeated the process (Brereton, 1981). The second method consisted of a contract system. A French creole, with more disposable capital than the typical peasant farmer, bought a large block of Crown lands, cleared it, and entered into an agreement with different contractors whereby each contractor was given three and one fifth acres on which to plant cocoa. When the trees were bearing, the capitalist reclaimed the land and paid the contractor an agreed upon sum for each tree. This method was beneficial for both parties. The capitalist was able to develop an estate cheaply and easily and the contractor could gain wages without an initial output. As a result of their privileged status as plantation owners, the

merchants and distributors of cocoa, the French creoles, dominated the plantation as well as the commercial side of the cocoa industry.

The rise of the cocoa industry was inextricably connected to the economic renaissance of the colored French creoles. With the abolition of slavery and a growing acknowledgement of civil rights around the world, the colored creoles were no longer content to accept the oppression of the past. After years of domination and marginalization, the colored French creoles had the economic and socio-political opportunity to ascend the social ladder; they were determined to obtain and maintain an elevated position. With the capital gained from the cocoa industry, and their recovered and/or newly gained social status, coloreds enjoyed a renewed period of prosperity; they also began living lavish lifestyles that were a testimony to their wealth. Thus, after years of persecution, coloreds needed to affirm their status in society. Consequentially, they invested in the asset that was most representative of their identity and would reach the greatest audience - their homes.

Pre-cocoa boom, the houses of the elite, though large in scale, were simple in design. Wealthy homes had European features such as a mansard roof, dormer windows and loggias but lacked ornamentation or any distinguishing features. The emergence of a new elite group of cocoa planters and merchants, however, brought a profound and long-lasting change to the residential fabric. With their newly acquired capital, the new elite built mansions at a level of extravagance that had never before graced the island. French creole colored planters and merchants now had the capital to live the life of a French aristocrat with “all the pretensions of a count” (Brereton, 1981). In the country, they built lavish estate houses such as the La Chance estate built in 1880 by Gaston de Gannes, one of the pioneers of the rebirth of the cocoa industry in the 1860s. At two stories, La Chance was a timber affair equipped with a marble stair entrance

and porte-cochère (Lewis, 1983). However, the truly extravagant display of the cocoa planters and merchants consisted of the town houses that were constructed around the Queen's Park Savannah in the Port-of-Spain.

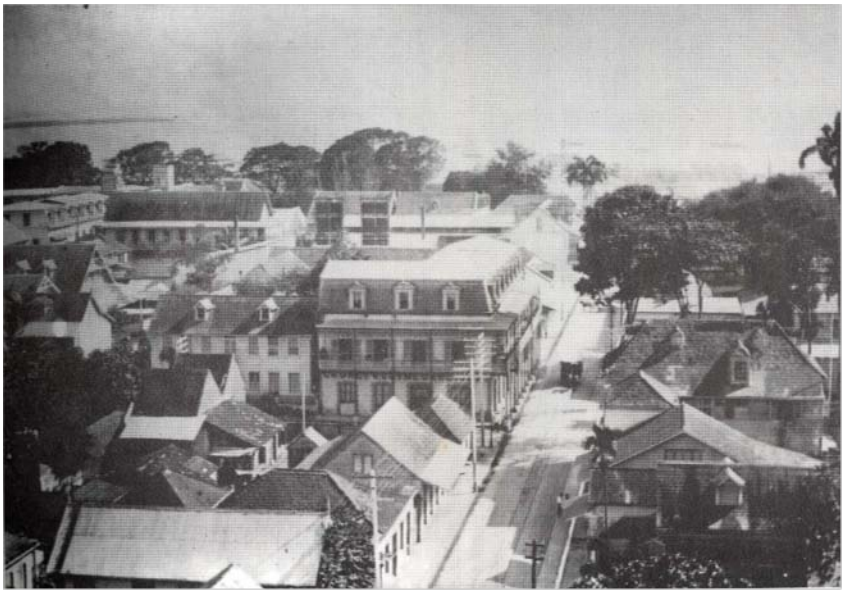

Figure 1. Overhead view of St. Vincent Street Port of Spain taken in the 19th century. This image illustrates the French style of building. Focal buildings in the photo possess mansard roofs, dormer windows and quoins. By G. Besson, 1985, *A photographic album of Trinidad*, 51.

Figure 2. La Chance Estate: One of the elaborate plantation houses of the late 19th century. By G. Besson, 2008 *Our Built Heritage*.

What the Nouveau Bourgeoisie Built

Trinidad had the perfect socio-cultural environment by the mid-nineteenth century to support the development of eclecticism. Trinidad was populated with Creoles, local-borns descending from immigrants of Venezuela, Scotland, England, Ireland, France, Spain, parts of Africa, and many other countries. With this mélange of ethnicities, Trinidadians described their new homes as follows:

> A place conducive to a diversity of culture and expression. Indeed, the arts in Trinidad including its architecture, confirm a propensity toward the bringing together of numerous influences. It is a collagist expression bringing together multiple parts, reconciled in a cohesive "whole". This is the nature of its people and the inclination of its artistic production. (Cazabon, 2011, p. 12)

It is from this collagist culture that the mansions around the 'Grand Savannah' were born.

Trinidad's 'Grand Savannah' or 'The Queen's Park Savannah' as it is now called, has been a hub of cultural activity since 1828. Approximately 260 acres of formerly agricultural land was sold to the *Cabildo*, the colony's governing body, in 1817 by the Peschier family. For many years, the site remained the grazing ground of cattle for the citizens of Port-of-Spain. However, by 1828 The Grand Savannah became a playground for ladies and gentlemen as well as the "place to be seen", with sports matches, horse races and tram rides. Thus, it became the perfect location to build a grand mansion to represent an individuals' success to the world. The land around the Grand Savannah was coveted because it offered a relief from the densely growing city. The elite clamored to obtain a bedroom window that would overlook the socially active park and to have their houses cooled by the cherished, Savannah breezes. It was not surprising then that by the turn of the 20th century, some of the islands' most successful cocoa planters and merchants built their magnificent residences along the western side of the Savannah.

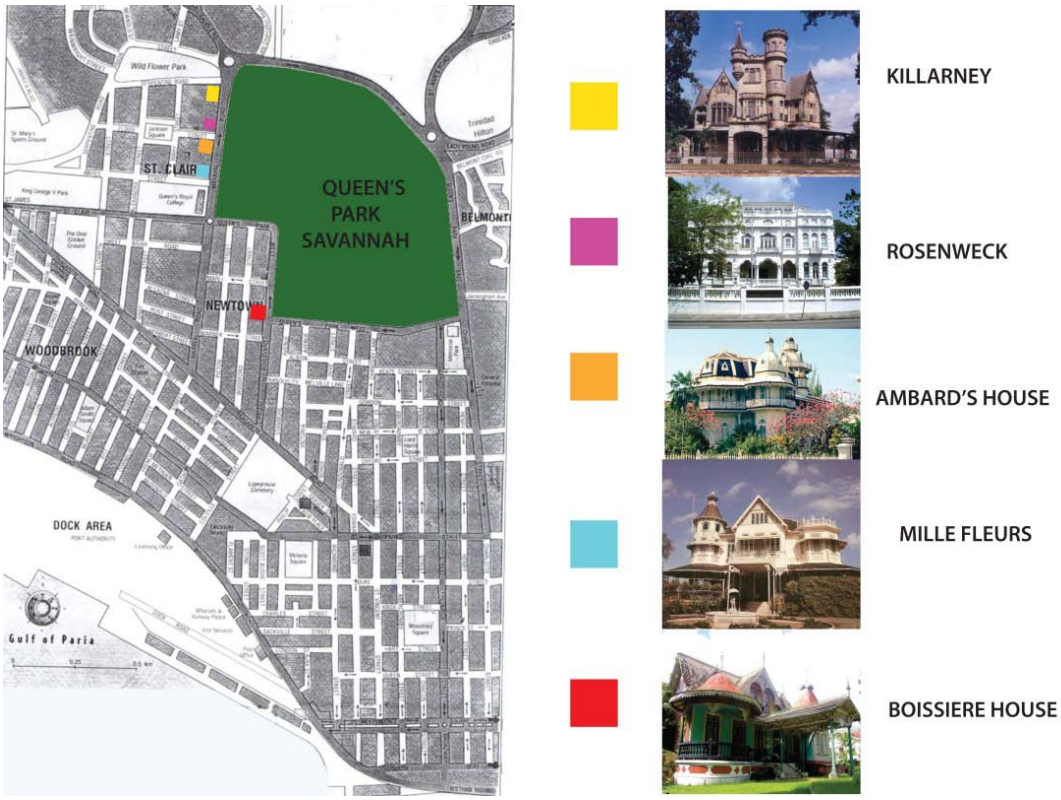

Figure 3. Map of Port of Spain showing the location of mansion of the elite along the Savannah Source: Composition by author. Pictures used by G. Maclean, 2011, *Residential.*

By 1904 the land to the west of the Savannah along Maraval Road included a series of mansions characterized by randomly assorted European styles. To design these luxurious homes, architects reproduced European designs (mainly British and French but also Italian, Dutch, and Moorish designs) and complemented it with indigenous peasant design. Each house had its own distinct style intended to outshine its grand neighbor. Killarney, or Stollmeyer's Castle, commissioned by Charles Fourier Stollmeyer, was the first house to be built bordering the Savannah. Designed in 1904 by a Scottish architect, Robert Gillies, this turreted residence was reminiscent of the German Romantic style and was fashioned after a wing of the Balmoral Castle built by Queen Victoria and Prince Albert in 1856 in the Highlands of Scotland.

Figure 4. Killarney (left) and Balmoral Castle (right). Killarney was designed in 1904 and the first of the mansions around the Grand Savannah. Balmoral Castle in Scotland was the inspiration for Killarney. By G. Maclean, 2011, *Residential*.

Following the construction of Killarney, Joseph Leon Agostini built the Rosenweck house (known as Whitehall today) with white coral limestone from Barbados; this style was reminiscent of the Moorish Mediterranean architecture of Corsica, a French island in the Mediterranean Sea from which the Agostini family originated (Watterson, 1998).

Figure 5. Rosenweck (left) and La Tunisienne (right). La Tunisienne, was a villa in Hyeres (a seaside French town) influenced by Moorish architecture. Architectural works like La Tunisienne influenced Rosenweck. By G. Maclean, 2011 *Residential.*

The Ambard's house (or Roomor as it is now called) was also designed in 1904 by a French architect for Lucien F. Ambard, a rich merchant (Watterson, 1998). The flamboyant house was inspired by the French Baroque style, with most of the materials imported from France.

Figure 6. Ambard's House (left) and The Château de Vaux-le-Vicomte (right). The Château de Vaux-le-Vicomte is a baroque French chateau located in Maincy, French. Architectural works like this influence Ambard's house. By G. Maclean, 2011, *Residential.*

Finally, in 1904 Mrs. Prada commissioned 'Mille Fleurs' as a gift for her husband, Dr. Enrique Prada (Watterson, 1998). The house was designed by local architect George Brown; Dr. Prada also took a special interest in the design. The house, designed like an English country house, was very conservative compared to its neighbors.

Figure 7. Milles Fleurs (left) and A villa in Forges-les-Eaux (right). The villa in Forges-les-Eaux, is designed in the French country house style that influenced Mille Fleurs. By G. Maclean, 2011, *Residential. Architecture in France 1800-1900*, 36-4.

The Boissière House

This agglomeration of ornate Euro-inspired mansions along Maraval Road was certainly a grand affair, and it was here, in 1904 that colored cocoa merchant Charles E.H. Boissière commissioned his statement piece the Boissière House (Watterson, 1998). Charles Boissière descended from an African slave and a rich French Creole planter who settled in Trinidad in the late 18th century. After acquiring wealth in the cocoa industry, Boissière traveled to England in the 1890s and observed the Grand Exposition in Britain. One of the features of the exhibition was the fashionable *Chinoiserie* artwork (Besson, 2011). *Chinoiserie* is a French term signifying "Chinese-esque"; it referred to the Chinese influence on European art and architectural designs at the time. Boissière recorded the Chinoiserie exhibition and returned to Trinidad with this inspiration. Along with his friend, builder Edward Bowen, he designed the Boissière house as a surprise for his wife, Alice (Besson, 2011). As a summary of his life, this house was an opportunity for Boissière to reflect his personal history, aspirations, local roots and travel abroad in his home.

Figure 8. The Boissière House. By L. Welcome, Jan 2010.

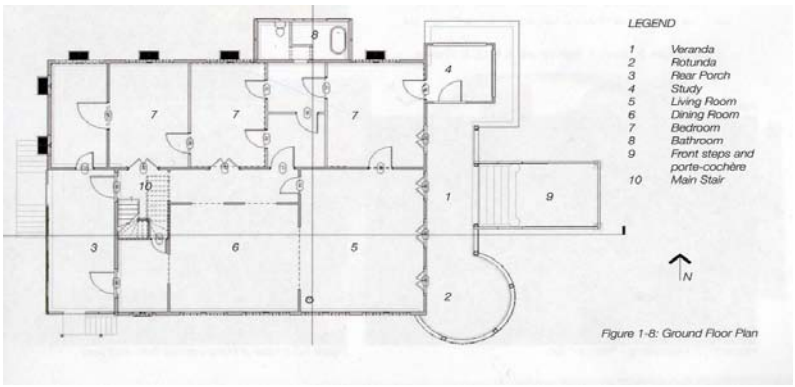

Figure 9. The plan of the Boissière House. By Cazabon & Ottley, 2011.

The house at No. 12 Queen's Park West, located at the southwest corner of the Savannah in New-Town Port-of-Spain, was modern for its time. Like other homes of the 1900s, the Boissière House possessed intricate fretwork, steep gables, complex roof forms with slate roofing, a central veranda, and cast iron fencing. However, the Boissière House combined these elements in a more picturesque and playful way than the others. For example, it was built using a technique called nogging, whereby a timber-studded frame was built, then in-filled with lime-cement and rubble, and finished off with a lime plaster. On the side façades of the house, the plasterwork was textured with aggregate and fashioned to resemble natural, cave-like, stone textures. Courses were scratched into the plasterwork to imitate a historical and authentic look. This façade treatment that imitated stone was not simply a fashionable addition; by imitating a more exclusive and expensive material counterpart, the status of the concrete- and its owner- became elevated.

Figure 10. Side façade of the Boissière House. In this photo some of the plasterwork is removed to show the use of nogging below. By L. Welcome, Jan 2010.

On the front façade, the concrete plaster was not altered to imitate stone but was instead left smooth and painted in colors that were meant to catch the eye and give a magical appeal to the house. The basic form of the house was a rectangle, with the street façade along one of the shorter sides of the rectangle. From the street façade, a study projected on the right side and a rotunda on the left side.

Between the rotunda and the protruding study was a porte-cochère, a porch-like structure, typical of 18th and 19th century mansions, that protected occupants from the elements as they dismounted the carriage. Above the porte-cochère loomed an exaggerated gabled dormer-window, which was one of the most defined components of the exterior image. The projecting volumes of varying shape, height and size brought great depth to the façade, giving it a sense of animation. All of these features were meant to draw an audience for admiration.

Figure 11. Front view of the Boissière House. By G.Maclean, 2011, *Residential.*

The main roof that capped the house was a steeply pitched gable form with wooden ridges running east to west and covered with green slate. The steep pitch of the roof accommodated an additional floor and cast-iron decorative crestings capped the ridge of the roof. Intersecting the main roof was a large dormer window; its rafters run north to south, perpendicular to the main roof. The large dormer window was flanked by smaller, non-functional, gabled roof projections on each side that added visual interest to the roof. The large dormer gable was decorated with fretwork; a decorative feature formed from intricately carving wood, using a jigsaw, to form a lacy pattern. The smaller dormer windows were also capped by lacy wood-work. The fretwork not only served as a decorative motif but also had practical functions; for example, it filtered harsh sunlight, thereby allowing a cooler interior with a soft

glow. The fretwork also created a magical lighting effect at night as it diffused the light of the lantern on the interior, creating a visual experience of twinkling lights on the exterior. The use of this fretwork was meant to directly reference a European heritage as it was popularized in Europe during the Victorian era and could be seen in works such as 'Les Dunes', a villa in Chatelallon-Plage, France (Lemoine, 1998).

Beneath the larger dormer was a porte-cochère; a feature of many late 18th and 19th century European mansions. The 14-foot wide porte-cochère had a functional aspect to protect one from the elements as they disembarked from a carriage ride and proceeded to enter the house. The porte-cochère was a symbol of class, implying the need for protection of the prestigious from the elements, a luxury that was not afforded to the servants. In the Boissière House the porte-cochère was reinterpreted to give it a lighter and daintier effect than traditional European houses. Heavy columns were replaced by thin fluted cast-iron posts. What would have been a dense architrave was instead a series of intricately carved, thin wood panels. The rafters that comprised the roof of the porte-cochère were exposed on the underside, and again, the rafters were capped by decorative wooden fretwork. All the features together contributed to a light and airy feel.

Figure 12a. Porte-cochère in a European context. Source: http://www.britannica.com/EBchecked/topic/471059/porte-cochere

Figure 12b. Porte-cochère in a Trinidadian context. Source: Welcome, Jan 2013.

During this time, most of the land was owned by the Crown Colony. With the uncertainty of the time period of which they would have possession of the land, a resident would build his house supported off the ground on concrete blocks. The house did not touch the land and, subsequently, could be transported off the land as necessary. The use of a concrete foundation, with its implications of longevity, meant that one owned land, and, by extension, one had a certain economic level to afford the land. Therefore, the concrete base of the Boissière House was a status symbol. This message was further reinforced by the exaggeration of the depth of the base and the red decorative detailing placed against a white backdrop. The meticulous detailing of the base attracted attention and alerted the viewer that the ornate jewel, which was the Boissière House, was a permanent fixture in its landscape.

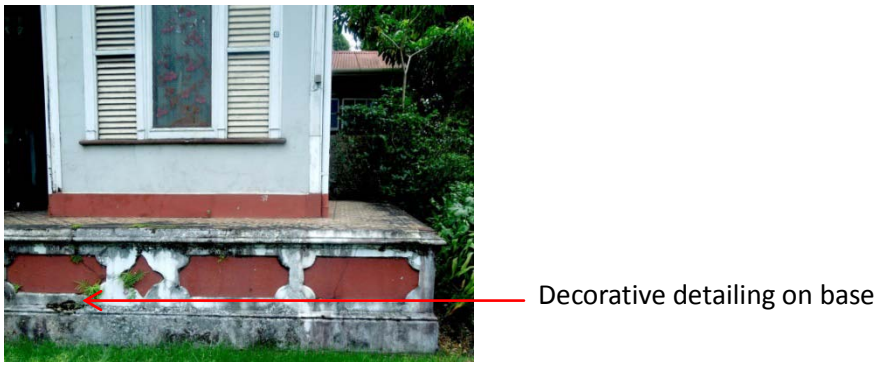

Figure 13. Base of the Boissière House. By L. Welcome, Jan 2013.

The veranda was placed at the front of the house, reflecting Trinidad's Spanish and French heritage. The French and the Spanish had a preference for verandas located in the front, facing the street, because of their preference for public interaction. The stairs leading up to the veranda were made of large single slabs of marble imported from Italy. The floor was decorated with multi-colored, ceramic tiles from England with an ornate, geometric pattern.

Figure 14. Veranda with geometric floor tiles. By L. Welcome, Jan 2013.

The importation of fine, foreign materials from Europe was yet another way to set oneself apart from the average person. To cover the veranda, a shed roof supported by thin cast-iron columns was used. These columns were topped with decorative, floral, fretwork capitals, made

of wood, which were a reinterpretation of Classical language. The veranda and the rotunda located at its west side were enclosed by a concrete balustrade, painted black, of Classical influence. The rotunda and the projecting study were capped with pagoda-like roofs of sheet metal inspired by the *Chinoiserie* exhibits C.E.H Boissière visited in Europe. The apex of the roof was covered with a cast-iron finial reminiscent of art-nouveau finials. Overlapping the oversized dormer, these unique pagoda-like rooflines, flanked by mini gables, all back-dropped by the main east-west running gable, came together to create a complex and dynamic roof silhouette.

The doors and windows of the Boissière house presented another opportunity to add more decorative flare. At the front of the house there were four sets of double doors each of same height and width (9'6"x 4'). Each door had an inset, arched, frosted, glass panel engraved with art-nouveau inspired, decorative floral patterns. Around the doors were six-inch wide wooden moldings painted white to stand out against the natural wood palette of the doors. Above the doors were ventilation panels called 'fanlights' constructed with intricately carved wooden panels. There was a single, side-door that led to the protruding study; inset in this side door was a stained-glass panel painted with a floral motif also inspired by *Chinoiserie* artwork.

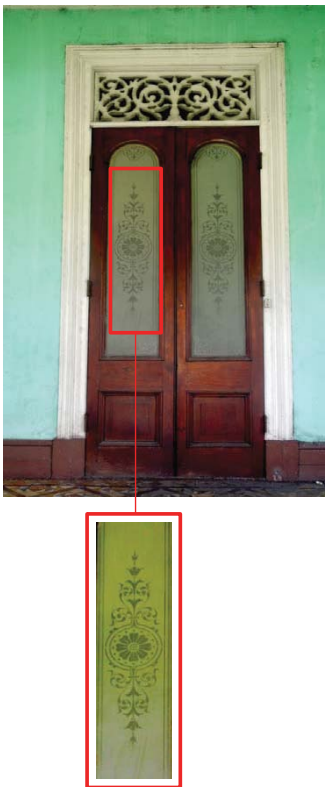

Figure 15. Main entry door with Art Nouveau detailing. By L. Welcome, Jan 2013.

Figure 16. Study door with Chinoiserie artwork. By L. Welcome, Jan 2013.

The typical windows of the house consisted of central double hung windows with frosted glass in a wooden sash. The glass was surrounded on both sides by jalousies (louvers). The glass and the jalousies were separated by wooden trim, painted red and fashioned to look like stone coursing. Below the sill was a wooden molding painted white. The window of the over-sized dormer was an inversed composition of the typical window of the house. In this window, the arched louvered panel was placed in the center, with arched glass window panels at its sides. Again, the wood trimming was painted red and imitated stone coursing.

On the front elevation, the study also had two signature windows. The first window, like the others, consisted of three vertical sections, a central stained glass panel with a similar Chinese inspired, floral motif, painted on it to match the motif on the door, and louvered panels on either side. The vertical panels were separated by wooden moldings painted white and carved

to look like engaged pilasters. Above this window was an oval shaped window of stained glass also decorated with a floral motif. The window was framed by a white molding above which were offset wooden, decorative eye-lash details. The curve of the eave of the pagoda-like roof that capped the study framed the oval window. The pagoda roof of the study and the oval window provided an interesting visual juxtaposition. The eave of the roof resembled the brim of a hat, and this metaphor was reinforced by the eyelash detailing added to the top of the oval window connoting an eye, that gave an anthropomorphous quality to the protruding study volume. The hat reflected another status-reinforcing symbol of the era. Diana Crane theorized that until the 1960s, hats were the most important article of clothing to indicate social distinction among men in Europe and North America (Crane, 2000). According to Crane, hats were less expensive than other clothing articles of distinction, so they provided the ideal opportunity for visually blurring traditional class boundaries. Certain hats became associated with specific social strata, thereby making hats an important marker of class boundaries. This meant, according to Crane, that men could use hats to claim and maintain social status. The steep pagoda-like roof of the study with its hat-like image functioned in a similar way to the hat worn by men of the 19th and early 20th century. It is a timeless indicator of class and distinction that sat on the head of the study volume.

At the front of the property was a short fence that allowed visual connectivity from the veranda to the Savannah. However, it demarcated boundary, acting as a physical and visual division between the interior elite and exterior “others”. The fence consisted of a stone-faced, three-foot high wall that was two feet wide, the top of which had a beveled edge. Running the length of the wall, above the layer of stone, was a layer of ornate cast iron work approximately three feet high. The iron-work was light and transparent and contrasted with the heavy, solid

stone wall. At the end of the fence were two six-foot high plastered piers, topped with capitals that served to support the grand double cast iron gates.

Upon examining all of the disparate features of home exterior, it becomes evident that this playful collage-like work cannot be tied to any specific style. There were references to the growing movements in Europe that represented renewed appreciation for the decorative arts. Two of the most influential were Arts and Crafts in Great Britain and Art Nouveau in France. The Arts and Crafts movement combined finely crafted simple forms with applied decorative details. Art Nouveau deviated from the classical idea of ornament as an applied component. Instead, the style embedded a nature-inspired ornament within the limits of the structure so that it became an essential part of the design. There were also references to High Victorian and Oriental precedents in the Boissière House. This house is described as elegant because it was the culmination of a marriage between local building techniques and European architectural influences. It is thus a fine exemplar of the early 20th century, Trinidadian house condition that sought to embody class status and recognition. Though it is one of the smallest of the houses that line the Savannah, it sought to compensate through ornamentation. No surface of the house was left unadorned, and it married these different accents to create a fanciful showpiece, which vied for attention on the grand stage of competing mansions. Practical components were fashioned to become ornate. For example, simple materials such as wood and concrete were textured and transformed to imitate extravagant stone. Color was used in a strategic manner to draw the eye to specific details. All elements were combined in an intelligent way such that they complemented each other, leaving new details to be discovered with every glance.

Although these five mansions were constructed in the same year, they differ radically from a stylistic perspective. John Newel Lewis, in discussing the reason for the occurrence of

these diverse hybridized mansions, each grander than the next, developed the 'Queen of the Bands' theory (Lewis, 1983). Carnival was introduced to Trinidad in 1785 with the arrival of the French Creoles. The festivities include the parade of various bands throughout the street, consisting of costumed revelers. Each band had a Queen, a person dressed in an extravagant costume, leading the band to dazzle spectators. The various 'Queens of the Band' sought to be more magnificent than the next as they were placed against each other in competition on a single stage. They were judged according to craftsmanship, color and originality. According to Lewis, it is the spirit of the Queens of the Bands that is contained in the mansions around the Savannah. Each mansion competed against the other in terms of craftsmanship, décor and originality for the title of most magnificent on the Savannah stage.

Influence of the Nouveau Bourgeoisie Mansions

As opposed to the isolated plantations on the outskirts, these Grand mansions allowed the elite an opportunity to flaunt their wealth to an audience. The audience did not only consist of elite competitors but also of an emerging stratum of middle-class coloreds and blacks aspiring to obtain a similar status. People of all classes traveled everyday along the Maraval Road and partook in the leisure activities that occurred in the Savannah. Also, the then working-class neighborhoods of Woodbrook and Belmont were located in close proximity to the Savannah. As this middle-class group came in contact with the ostentatious mansions, they became enthralled by their mesmerizing grandeur. As a result, their stylistic influences extended beyond the homes of the nouveau bourgeois to the homes of the humble as the middle-class emulated aspects of the mansions in their own houses.

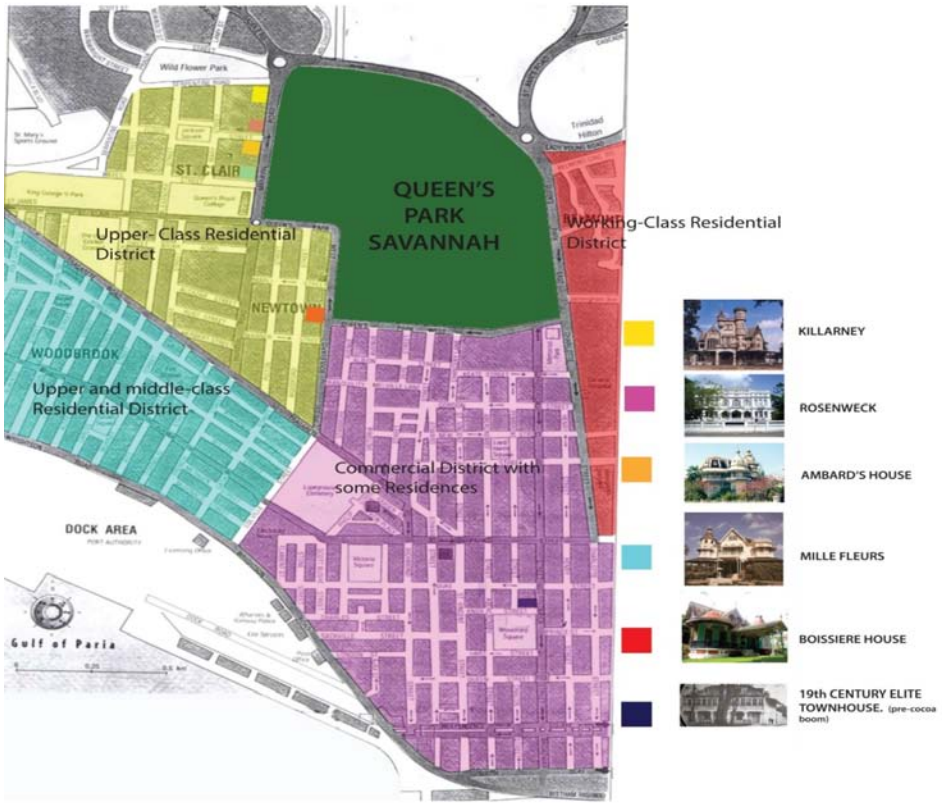

Figure 17. Map of Port of Spain showing the class distribution. By L. Welcome, 2012.

After emancipation, the middle class expanded due to newly liberated, ambitious coloreds and a few blacks rose up the social ladder through their concerted efforts to become educated (Brereton, 1981). They did not have the advantage of skin color like the white creoles nor did they have a legacy of wealthy slave-owning ancestors as did the French creole coloreds. If these newly liberated people wanted to attain respectability, it was to be self-made. Many ex-slaves moved to Port-of-Spain and other urban areas where schools were more readily available so that their children could be educated. The education system developed in Trinidad after 1838 offered an escape from "the harshly restrictive world of the manual laborer" (Brereton, 1981). By 1870, an Education Ordinance was passed that set up a dual education system of state-aided denominational schools existing side by side with government schools in every ward of Trinidad (Brereton, 1981). Both types of schools at the elementary level were open to any child

regardless of race, wealth, or religion. Black children, especially in the urban areas, obtained an education, thereby allowing them to rise above wage labor jobs to become artisans, small shopkeepers, minor civil servants, and store assistants, and achieving a lower middle-class economic status. While secondary school education remained an institution exclusively for the upper-middle class and the elite, there was one opportunity for children of the lower economic status to attend this institution. Every year, the secondary schools had an 'exhibition' whereby a scholarship was offered to a lower-income male from the government-funded or government-aided primary schools. This scholarship system opened up secondary school educational opportunities to a small number of black and colored males of lower-income families. This education offered them the opportunity to vie for white-collared jobs such as teaching, journalism, the civil service, as well as minor positions in business such as sales clerks within commercial cocoa stores. The white-collar jobs also reflected western-cultural values and norms and, hence, helped them gain the respectability of their former masters.

With their new jobs, the middle- and lower-economic status men acquired property upon which to build their homes. However, they began to wonder what their houses should look like. While the white-collar jobs did not afford them much disposable income to build the elaborate mansions of the elite, it was also no longer sufficient to live in a simple chattel house if they wanted the respect of the socialites that lived around the Grand Savannah. Thus, the newly liberated men had to find a new aesthetic that would signal their new position in society.

In analyzing the houses of the elite, the men deciphered that the things that made these houses special, the reason they caught your attention and stood out among all others, was the attention the designer paid to ornate details. Thus, it was the ornamentation that took the house from the realm of the ordinary and transported it to the realm of the fanciful and grand. While

middle-income families could not build expansive houses of stone with turrets, they could, however, emulate the ideas of class and beauty reflected in the elite mansions on a smaller scale. To design these houses, they borrowed from architectural expression of the elite to create culturally conscious designs mimetic of grander urban houses like the Boissière House. The typical house of the urban middle-class was a one-story, wooden dwelling with a simple, thin, rectangular form within the dense urban fabric. At the front of these houses was usually a veranda and porte-cochère directly referencing those found in the grander mansions. With the simplicity in form, it was the detailed accents that brought complexity and charm to the house. Decorative wooden fretwork, originally promoted by Scottish architect George Brown, became a prominent stylistic trend and one of the most commonly used forms of ornamentation of the middle-class house.

George Brown's most important contribution to Trinidadian architecture was his use of standardized prefabricate in the realm of residential architecture. He standardized and mass-produced doors, windows, railings, jalousies, window units, crestings, finials, balustrades, cornices, skirtings, and fretwork barge boards (Lewis, 1983). These functional components were given an aesthetic quality so they would have both practical and ornamental functions. Under the direction of George Brown, many workshops opened in the Port of Spain area and mass amounts of standardized building components were prefabricated. With the invention of the jigsaw in 1865, the process of making intricate fretwork out of wood was revolutionized; as a result, these workshops produced miles of fretwork (Besson, 2011). The mass production of these standardized building components meant one important thing; members of the middle-class could now afford designed components that brought an aesthetic quality to their practical needs. These functional, yet decorative features soon became essential to the composition of the typical

residential house, eventually becoming institutionalized. The term 'Gingerbread house' was coined to describe these houses. The fretwork, crestings, finials, cornices, and skirtings together decorated the simply designed house, providing a sense of respectability that its owner craved. When referring to the Gingerbread house, Lewis described it as "a unique combination of decoration and practicality" (1983, p. 201). Though these houses were small in scale, their intricate detailing made their stature un-mistakable.

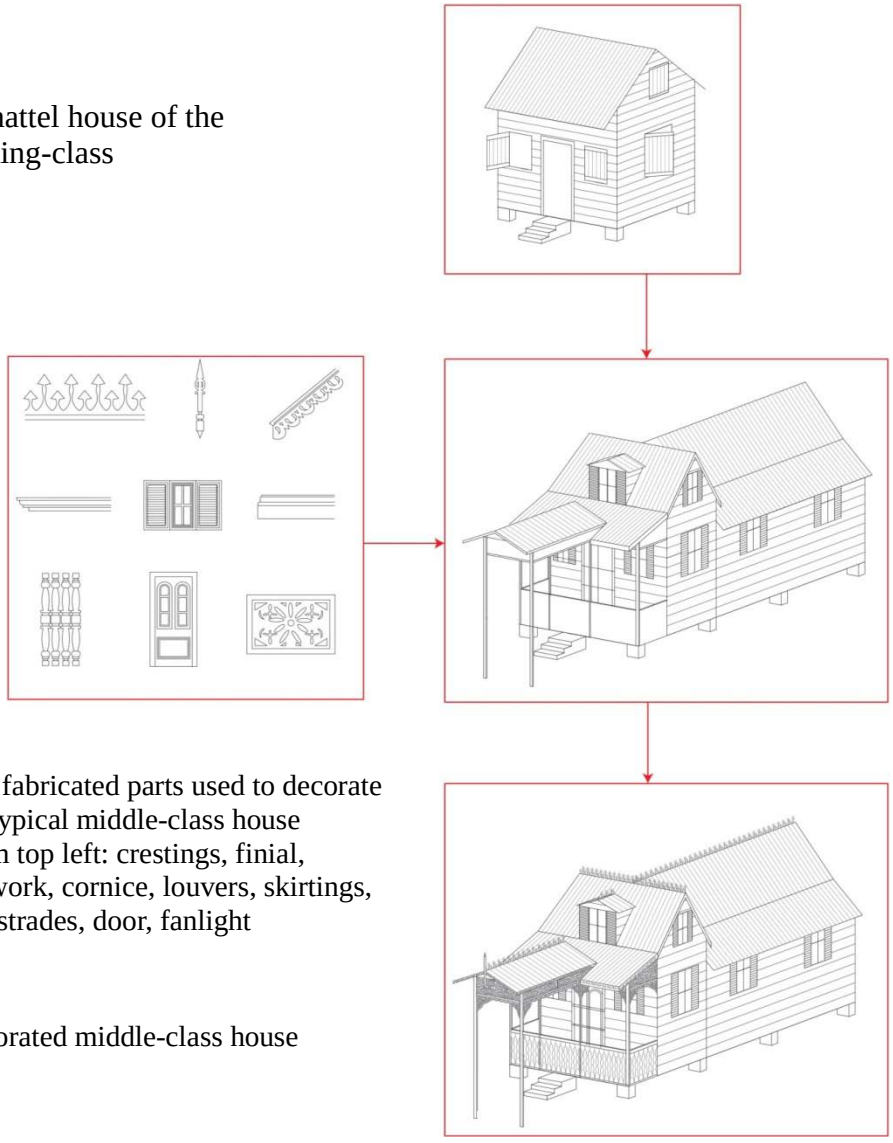

Figure 18. Diagram showing how the use of ornament transformed the middle-class house. By L. Welcome.

Figure 19. Typical early 20th century middle-class houses. By L. Welcome, Jan, 2013.

Although the houses of different class levels, at the beginning of the 20th century, were visually different, they were of one architectural lineage. The influence was a cultural one rather than a purely stylistic one. The houses across economic class levels all borrowed from external precedents, but combined them with local traditions and ornamentation to transform them from the realm of the banal to the realm of the respectable and enviable. Each house shared in a common goal - to create an artifact that spoke of its owner's elevating position as they strove to differentiate themselves in the growing classist and capitalist environment that was early 20th century Trinidad.

References

Besson, G. (2008, February 16). Our built heritage [Web blog post]. Retrieved from http://caribbeanhistoryarchives.blogspot.com/2008/02/our-built-heritage.html

Besson, G. (2011, August 23). The queen's park Savannah [Web blog post]. Retrieved from http://caribbeanhistoryarchives.blogspot.com/2011/08/queens-park-savannah.html

Besson, G. (1985). *A photographic album of Trinidad at the turn of the 19th century*. Port of Spain: Paria Publishing Co Ltd.

Brereton, B. (1981). *History of modern Trinidad, 1783-1962.* London: Heinemann.

Cazabon, Y. P., & Ottley, A. (2011). *A tale of two houses - Vol.1: An historical record of the Boissière and Piccadilly houses, Port of Spain, Trinidad and Tobago*. Ottawa, Canada: Carleton University.

Crane, D. (2000). *Fashion and its social agendas: Class, gender, and identity in clothing.* Illinois: University of Chicago Press.

Lemoine, B. (1998). *Architecture in France 1800-1900.* Translated by Alexandra Bonfante-Warren. New York, NY: Harry N. Abrams.

Lewis, J. N. (1983). *Ajoupa*. New York: AIA Service Corporation.

Maclean, G. (2011, November 15). *Residential*. Retrieved from http://citizensforconservationtt.org/main/index.php/builtherit/bhresidential

Watterson, G. G. (1998). *This old house: A collection of drawings of Trinidadian homes*. Port of Spain: Paria Publishing Co Ltd.